Hindawi
International Journal of Energy Research
Volume 2024, Article ID 8837343, 27 pages
https://doi.org/10.1155/2024/8837343

Research Article

Catalytic Efficacy, Kinetic, and Thermodynamic Studies of Biodiesel Synthesis Using *Musa* AAA Plant Waste-Based Renewable Catalyst

Bidangshri Basumatary,[1] Alpaslan Atmanli,[2] Mohammad Azam,[3] Siri Fung Basumatary,[1] Sujata Brahma,[1] Bipul Das,[4] Sanfaori Brahma,[5] Samuel Lalthazuala Rokhum,[6] Kim Min,[7] Manickam Selvaraj,[8,9] and Sanjay Basumatary[1]

[1]*Department of Chemistry, Bodoland University, Kokrajhar 783370, Assam, India*
[2]*Department of Mechanical Engineering, National Defense University, Ankara 06654, Türkiye*
[3]*Department of Chemistry, College of Science, King Saud University, PO BOX 2455, Riyadh 11451, Saudi Arabia*
[4]*Chemical Engineering Division, CSIR-North East Institute of Science and Technology, Jorhat 785006, Assam, India*
[5]*Department of Chemistry, Gauhati University, Guwahati 781014, Assam, India*
[6]*Department of Chemistry, National Institute of Technology Silchar, Silchar 788010, Assam, India*
[7]*Department of Safety Engineering, Dongguk University, 123 Dongdae-ro, Gyeongju 780714, Gyeongbuk, Republic of Korea*
[8]*Department of Chemistry, Faculty of Science, King Khalid University, Abha 61413, Saudi Arabia*
[9]*Research Centre for Advanced Materials Science (RCAMS), King Khalid University, PO Box 9004, Abha 61413, Saudi Arabia*

Correspondence should be addressed to Sanjay Basumatary; waytosanjay12@gmail.com

Received 1 September 2023; Revised 20 December 2023; Accepted 22 December 2023; Published 24 January 2024

Academic Editor: Debabrata Barik

The study focuses on the preparation of an inexpensive, ecocompatible, and effective catalyst from the Bharatmoni (*Musa* AAA) plant for biodiesel synthesis using *Jatropha curcas* oil. The burnt ashes obtained from the Bharatmoni fruit peel, stem, and rhizome were calcined at 550°C for 2 h and characterized by analytical techniques. Utilization of CBS-550 catalyst achieved a higher yield of biodiesel (96.97%) within 12 min compared to CBP-550 (96.89% in 16 min) and CBR-550 (96.53% in 18 min) catalysts under optimum reaction parameters of 5 wt% of catalyst and 9 : 1 MTOMR at 65°C. This study described that catalyst having a higher concentration of potassium in its oxide and carbonate form has higher catalytic activity. The surface morphology of the prepared catalysts revealed mesoporous in nature. The kinetic and thermodynamic studies of the reactions catalyzed by the present catalysts follow the pseudo-first-order kinetic model exhibiting a nonspontaneous and endothermic process. The reaction catalyzed by the CBS-550 catalyst revealed the lowest E_a of 44.36 kJ mol^{-1} and is known to be the superior catalyst among the derived catalysts of this study.

1. Introduction

Currently, the rate of energy utilization is increasing continuously. The Energy Information Agency (EIA) projected that the world consumed 283 quadrillion Btu of energy in 1980 and currently the world is consuming around 596 quadrillion Btu, and with this increasing trend, the world may require 60% more energy by 2030, out of which 45% will be needed for China and India [1]. Most of the energies are derived from finite fossil fuels to date. Fossil-based fuels are the leading resource of energy which have been depleting for long years, and their reserves are remaining limited on the earth [2]. As a consequence of long-term fossil fuel usage, CO_2 and other polluting gas emissions have been drastically elevated which is the major factor of global warming and the consequence of today's climate change [3, 4]. Fossil fuels being the nonrenewable energy resources are expected to be completely used up in the coming future

maybe by 2050 [5]. Therefore, to avoid the energy crisis and to overcome the bad impact on the environment, many researchers have drawn their attention to study the production of alternate sources of energy. Looking at the alternate source of fossil fuels, researchers found biodiesel as an effective fuel that emits low exhaust gas like sulfur, HCs, and CO. Biodiesel is nontoxic, clean and environmentally friendly, renewable, and biodegradable having higher cetane number and flash point with excellent lubricity [6, 7].

Microemulsion, direct use of vegetable oil, transesterification, and thermal cracking are the four different methods for the preparation of biodiesel, and among these, transesterification is a simple and common reaction to produce it effectively [8]. In this reaction, the animal oils and vegetable oils such as edible or nonedible oils containing triglycerides undergo a reaction with a catalyst and alcohol producing the chemical product, methyl or ethyl esters known as biodiesel [9]. The catalyst has a noteworthy role in producing quality biodiesel and its yield percentage in variable reaction time depending on the employed catalyst. Researchers performed several tests with different catalysts and studied their effectiveness. Base homogeneous catalysts such as KOH, NaOH, CH_3ONa, and CH_3OK and acid homogeneous catalysts such as R-SO_3H, H_3PO_4, HCl, and H_2SO_4 are employed for biodiesel preparation [10, 11]. Homogeneous base catalysts are usually used for very fast reaction rates and mild reaction conditions but are not suitable for large-scale production, whereas homogeneous acid catalysts are very weak in catalytic activity and take longer reaction time. Both acid and base homogeneous catalysts are highly corrosive in nature, and purification of biodiesel yield requires a huge amount of solvent for several washes. Overall, biodiesel yields are reduced by the utilization of such catalysts and require more energy, and it is expensive. The use of homogeneous acid or base catalyst cannot be recycled [12]. In the literature, there are several enzymatic catalysts for biodiesel production. However, the enzymatic catalyst is very weak in catalytic activity, highly sensitive to alcohol and denaturation of enzymes and is highly expensive [13, 14].

Heterogeneous catalysts, *viz*., organosulphoric functionalized mesoporous silica, sulfated zirconia, nafion resins, tungsten oxides, and sulfonated saccharides [15], and solid base catalysts such as oxides of metal, mixed metal oxides, and hydrotalcite are utilized for the synthesis of biodiesel [16]. These heterogeneous acid or base catalysts needed high amounts of chemicals for synthesis and involve complex processes which increase the overall expenditure. Utilization of such catalysts has disadvantages such as catalyst's active site leaching that may affect in product contamination, also not environmentally friendly and nonrenewable [13, 17]. Some natural CaO-based heterogeneous catalysts are prepared from eggshells, animal bones, snail shells, mussel shells, crab shells, clam shells, waste chicken manure, and chicken and fish bones for the preparation of biodiesel [17, 18]. However, these catalysts are not preferred due to their complex methodology of preparation and moderate efficiency in producing biodiesel [19]. Therefore, the focus of the researchers has been shifted to economical and environmentally friendly catalysts derived from agrowastes having relatively high catalytic activities that can be employed for commercial production. These types of catalysts do not allow to form soap during the reaction and, hence, are easy to handle and separate, recyclable, widely available in nature, and considered sustainable [20]. *Carica papaya* [21], *Mangifera indica* peel [17], leaf of *Tectona grandis* [22], *L. perpusilla* Torrey [23], Poovan banana pseudostem [24], *Musa acuminata* flower petal [25], peels of orange [26], and *Musa acuminata* peel [27] were employed as raw materials for catalyst preparation and reported with variable catalytic activities in biodiesel synthesis.

A potential catalyst from agrowaste can be derived from the banana plant. Banana is one of the most extensively grown-up herbaceous plants in the world, cultivated in over 130 countries for fruit, producing about 16% of total global production of fruits [28]. India ranks first among the banana-producing countries, contributing 27% of the global banana production [28, 29]. After the postharvest of the total cultivated plants, 40% of the production remains as waste [30]. The peel, trunk, rhizome, rachis, leaf sheath, and peduncle part of the banana plant are the main waste materials. These waste materials have many applications depending on their chemical composition [31]. Some researchers reported the preparation of catalysts from banana plants and employed these in biodiesel production. Some of these reported catalysts are *Musa acuminata* peduncle [31], *Musa* "Gross Michel" [32], *Musa balbisiana* Colla peel [33], peels of *Musa paradisiacal* [34], peduncle of Pisang Awak [35], and K_2O-KCl based catalyst made from the peel of banana [36].

There are many varieties of bananas popularly cultivated in Assam, India. Banana plants have originated in India and the Eastern Asian region (Malaysia and Japan) [28]. Varieties of bananas have different origins from the same genus *Musa*, and it belongs to the *Musaceae* family. Human-edible bananas are derivatives of the *Australimusa* and *Eumusa* series [37]. Most of the edible bananas are a hybrid of the two wild diploid species of *Musa balbisiana* Colla and *Musa acuminata* Colla [28]. Mainly, banana comprises high concentrations of K along with other metals [33, 35, 38]. In this study, considering the nature of bananas, the postharvested banana waste was focused to generate a potential, effective, and cheap catalyst. The primary goal of the current study is to comparatively investigate the activities of the catalysts derived from the rhizome, stem, and peel part of Bharatmoni banana found in Assam (India) for the biodiesel preparation from *Jatropha curcas* oil and methanol via the transesterification process. Bharatmoni banana belongs to the AAA genome group [39]. Bharatmoni banana (*Musa* AAA) is widely grown in the northeastern part of India mainly in Assam. Its fruit peel color does not turn completely yellow even if it is ripened. The green color remains on the edges of the fruit even after ripening, and it has thick fruit peel. Commonly, its fruit length is around 13.75 cm and its fruit circumference is 10.20 cm. The Bharatmoni banana plant has mostly 6–7 hands per bunch bearing 78–90 fingers on it. As per another study reported by Saikia et al. [40], the Bharatmoni banana fills fruit within the lowest duration of 53.5 days than other varieties of banana. This

work reported the comparison of activities of the catalysts in biodiesel generation, reaction kinetics, and thermodynamic parameters along with chemical composition and reusability of the material catalyst prepared from Bharatmoni peel, stem, and rhizome. The determination of fuel properties of produced biodiesel was also reported. In this work, the post-harvested waste materials from the Bharatmoni banana plant were successfully turned into an effective catalyst that can be applied for the production of biodiesel at commercial scale.

2. Experimental

2.1. Chemicals and Materials. The Bharatmoni banana plant was collected from Kokrajhar, Assam, India, in February 2021. *J. curcas* oil was obtained from India Mart and used as a feedstock. The chemicals methanol (≥99.0%), n-hexane, petroleum ether (40-60°C), anhydrous Na_2SO_4, aniline, ethyl acetate (≥99.5%), silica gel G, ethanol (≥99.0%), phenolphthalein, and bromothymol blue were bought from Merck, Mumbai, India. The other chemicals like acetone (99%) were procured from Rankem, Maharashtra, India, and 4-nitroaniline was received from Loba Chemie brand, benzoic acid from APMI Limited, and Nile blue from Sisco Research Laboratories, India.

2.2. Preparation of Catalysts. After collection, the Bharatmoni banana plant was portioned out into three parts, *viz*., stem, peel, and rhizome (Figure S1). These three parts were cut again into small slices and dried under sunlight for 14-15 days. The dried rhizome, stem, and peel were combusted individually, and the completely charred ashes were obtained. The collected ashes were further calcined for 2 h at 550°C in a programmable muffle furnace, then stored in a desiccator, ground, and finally kept in an air-tight jar to use as a catalyst. In the present study, altogether six varieties of catalysts, three burnt catalysts and three calcined catalysts derived from the Bharatmoni, were explored in transesterification reactions, and these six catalysts were named and abbreviated as burnt Bharatmoni peel (BBP), burnt Bharatmoni stem (BBS), burnt Bharatmoni rhizome (BBR), calcined Bharatmoni peel at 550°C (CBP-550), calcined Bharatmoni stem at 550°C (CBS-550), and calcined Bharatmoni rhizome at 550°C (CBR-550).

2.3. Catalyst Characterization. To explore the characteristics of both calcined and burnt-derived catalysts from the banana plant Bharatmoni, sophisticated instruments such as XRD, XPS, FT-IR, HRTEM, BET, FESEM, and EDX were employed. The identification of crystalline materials of the catalyst was analyzed by powder XRD examination operating an X-ray diffraction (XRD) instrument (Rigaku). The detection of elemental compositions across the surface of the catalysts was done by X-ray photoelectron spectroscopy (XPS) (Thermo Fisher Scientific). The occurrence of numerous functional groups in the catalysts was identified by use of the Fourier-transform infrared spectroscopy (FT-IR) technique, between the wave number ranging from 4000 to 400 cm^{-1} using KBr as a matrix under the FT-IR spectrometer (Bruker). The catalyst was further investigated with HRTEM (JEOL, JEM2100 plus). The surface area, pore volume, and pore diameter were studied under Brunauer–Emmett–Teller (BET), Barrett–Joyner–Halenda (BJH), and N_2 adsorption–desorption isotherm technique (ASiQwin™ version 3.0). The elemental compositions and morphological surface structures of calcined catalyst (CBP-550, CBS-550, and CBR-550) samples were characterized with the help of energy-dispersive X-ray spectroscopy (EDX) and FESEM analytical techniques (Carl Zeiss NTS GmbH, Oberkochen, Germany). The burnt catalysts (BBP, BBS, and BBR) and 3rd recycled (CBS-550) samples were also investigated with the help of the same analytical technique to identify the chemical constituent and surface morphology using HV FESEM (Carl Zeiss, 05–07, UK). The pH value was determined for calcined catalysts (CBP-550, CBS-550, and CBR-550) by using calibrated pH meter (model number LT10). To determine the pH value, initially, the solution was prepared by dissolving 1 g of catalyst in 5 mL of distilled water, and then, the solution was dipped in an electrode of the pH meter. Thereafter, the solution is further diluted by adding more distilled water to make up the ratio as 1 : 5, 1 : 10, 1 : 15, 1 : 20, 1 : 30, and 1 : 40 (*w*/*v*), and the pH value of every ratio of a solution was determined. In addition, the basicity and soluble alkalinity of CBP-550, CBS-550, and CBR-550 catalysts were carried out as per the prescribed protocol [41].

2.4. Transesterification Reaction for the Biodiesel Synthesis. In the experiments, the reactions were set up by taking 2 g of *J. curcas* oil in a 100 mL of round-bottom flask fitted with a reflux condenser, allowing the reactants to be stirred (670–680) over a hot plate magnetic stirrer. The methanol and *J. curcas* oil were taken in different ratios (3 : 1, 6 : 1, 9 : 1, 12 : 1, 15 : 1, and 18 : 1) loaded with the prepared catalysts (CBP-550, CBS-550, and CBR-550) varying its wt% with respect to oil. Initially, the reactants were stirred for 3-5 min, and when the reaction temperature reached the desired temperature, the catalyst with the estimated amount was added. In this study, several experiments were carried out to investigate the optimum reaction conditions varying the reaction parameters. For the reactions, the temperatures were set at 35, 45, 55, 65, and 75°C using different catalyst wt% of 3, 5, 7, and 9. In order to observe the time of completed reaction, the stirring reaction mixture was checked by TLC (thin layer chromatography) with the solvent system of 20 : 1 *v*/*v* of petroleum ether and ethyl acetate. After the completion of the reaction, the mixture was filtered through a suction pump with the help of Whatman no. 42. The filtrate part is transferred in the separating funnel to extract adding pouring petroleum ether with vigorous shaking. The separating funnel was kept undisturbed allowing it to form separate layers. Afterward, the upper layer containing the product was collected in a clean and dry conical flask. The lower layer containing glycerol and some probable mixture of biodiesel part was again extracted 4-5 times. In the next step, anhydrous Na_2SO_4 was added to the extracted biodiesel and kept overnight in a conical flask. In the final step, this mixture was filtered and the filtrate biodiesel part was dried at 50°C using a vacuum rotary evaporator to

remove the solvent. The reaction of *J. curcas* oil was also studied by employing uncalcined catalysts (BBP, BBS, and BBR) and comparing their catalytic activities with the calcined catalysts. The yielded biodiesel was calculated with the following equation:

$$\text{Biodiesel yield}\,(\%) = \frac{\text{Weight of produced biodiesel}}{\text{Weight of oil taken for reaction}} \times 100. \quad (1)$$

2.5. Analysis of the Produced Biodiesel. The obtained biodiesel was analyzed by ^{1}H NMR spectroscopic technique (400 MHz, Bruker, Avance II) using $CDCl_3$ as the solvent. FT-IR spectrometer (Shimadzu, 00644) was used for recording FT-IR spectra of *J. curcas* oil and its transformed biodiesel. GC-MS technique (Perkin Elmer, 193 Clarus 680) was employed to determine the methyl ester compositions of biodiesel produced in this work. The equipment was operated by setting the initial temperature at 60°C for 6 min, and the temperature was raised at the rate of 5°C/min to 180°C and followed by increasing up to 280°C at 10°C/min. After maintaining the temperature again at 250°C, the sample was inserted to test having helium as carrier gas and the range of mass scan was from 20 to 500 Da. The source and transfer temperatures were 160°C and 180°C, respectively. The physicochemical analyses of the produced biodiesel such as density, cold filter plugging point, kinematic viscosity, pour point, and cetane number were performed at IOCL, Bongaigaon. The acid value (AV) of oil and biodiesel was obtained as per the procedure described [42], and from the AV, the free fatty acid (FFA) was calculated (FFA = AV/2).

Furthermore, saponification number (SN) and iodine value (IV) were measured by an empirical equation shown as follows [42]: $\text{SN} = \Sigma\,(560 \times A_i)/\text{MW}_i$ and $\text{IV} = \Sigma\,(254 \times D \times A_i)/\text{MW}_i$, where A_i is the percentage composition of individual component, MW_i is the molecular mass of individual component, and D is the number of double bonds in an individual component.

In addition, higher heating value (HHV), American petroleum index (API), cetane index (CI), aniline point, and diesel index (DI) were calculated using the standard equations recognized by American Society of Testing and Materials (ASTM) D2015 [43].

$$\begin{aligned}
\text{HHV} &= 49.43 - [0.041(\text{SN}) + 0.015(\text{IV})] \\
\text{API} &= (141.5/\text{specific gravity at } 15 \circ \text{C}) - 131.5 \\
\text{CI} &= 46.3 + (5458/\text{SN}) - 0.225\text{IV} \\
\text{AP} &= (\text{DI} \times 100)/\text{API} \\
\text{DI} &= (\text{CI} - 10)/0.72
\end{aligned} \quad (2)$$

3. Results and Discussion

3.1. Characterization of Bharatmoni Catalysts

3.1.1. Powder XRD Analyses of Catalysts. The XRD patterns (Figure 1) of CBP-550, CBS-550, and CBR-550 catalysts showed the existence of qualitative crystalline materials. In the probed data from XRD patterns, 2θ values were compared in accordance with JCPDS (ICDD 2003) and other reported data in published literature. In the X-ray diffraction pattern of CBP-550, the peaks at 2θ values of 28.41, 40.54, 50.18, 58.72, 66.44, and 73.88 showed the existence of KCl. The peaks obtained at 2θ values of 26.76, 29.79, 30.89, 31.99, and 34.75 referred to the presence of K_2CO_3 in CBP-550. The occurrence of K_2O in CBP-550 was affirmed from the characteristic peak at $2\theta = 39.43$. The peaks at 2θ values of 25.74, 28.50, and 38.61 represented the existence of SiO_2 in CBP-550. The peaks obtained at $2\theta = 32.82$, 30.62, and 44.95 correspond to the existence of CaO, SrO, and $CaMg(CO_3)_2$, respectively, in the CBP-550 catalyst. Therefore, from the XRD patterns of the CBP-550 catalyst, the components in the catalysts are revealed to be KCl, K_2CO_3, K_2O, SiO_2, CaO, SrO, and $CaMg(CO_3)_2$. The sharp peaks with high intensities were identified at 2θ values of 28.27, 40.46, 50.32, 58.59, 66.30, and 73.95 which attribute to KCl component present in the CBS-550 catalyst. The presence of K_2CO_3 in CBS-550 was detected by the peaks at $2\theta = 29.65$, 29.93, 31.31, and 31.86. The existence of K_2O was identified from 2θ values of 39.25, and the peaks at $2\theta = 32.13$, 32.68, and 43.15 clearly denoted the occurrence of CaO in CBS-550. The existence of SiO_2 in the CBS-550 catalyst was described by a diffraction pattern (Figure 1) at 2θ values of 25.63 and 28.55. $CaMg(CO_3)_2$ also existed in the CBS-550 catalyst which was revealed by the characteristic peak at $2\theta = 45.36$. Except for SrO, the same components also existed in CBS-550 compared with the CBP-550 catalyst. Similarly, the catalyst CBR-550 has a KCl component which is revealed by the peaks at $2\theta =$ 28.21, 40.50, 50.25, 58.74, 66.30, and 73.98. The occurrence of K_2CO_3 in CBR-550 was interpreted from the 2θ values at 26.55, 29.58, 30.14, and 32.06. The K_2O in CBR-550 was characterized by the peaks at $2\theta = 39.30$ and 48.60. The existence of CaO in CBR-550 was also established from the peaks at $2\theta = 32.61$ and 43.06. The characterized peaks at 2 $\theta = 25.73$ and 28.48 are due to SiO_2, at $2\theta = 33.72$ due to $CaCO_3$, and at $2\theta = 45.34$ due to $CaMg(CO_3)_2$ present in CBR-550 catalyst. Hence, the XRD analysis results explained that the CBP-550, CBS-550, and CBR-550 catalysts are mainly composed of carbonates and oxides of K, Ca, Si, and Mg which are significantly exhibiting high basicity. The obtained XRD results of the present work are well comparable with XRD data reported in other agrowaste materials, *viz*., Poovan banana pseudostem [24], *M. acuminata* peel [27], *M. balbisiana* Colla peel [33], *Carica papaya* peel [44], waste passion fruit peel [45], potato peel [46], and waste *Mangifera indica* peel [17].

3.1.2. FT-IR Analyses. The FT-IR analyses were conducted for CBP-550, CBS-550, CBR-550, and the 3rd recycled catalysts, and the spectra were are in Figure 2. The bands that appeared at the wave number of 3482 cm^{-1}, 3485 cm^{-1}, 3478 cm^{-1}, and 3437 cm^{-1} are assigned to stretching vibration of the -OH group in the CBP-550, CBS-550, CBR-550, and 3rd recycled catalysts, respectively. These indicate the adsorption of water molecules on catalyst's surface [20].

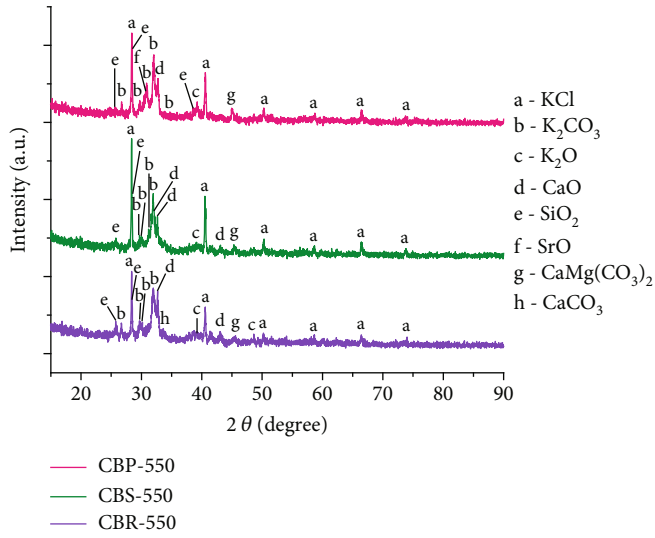

Figure 1: XRD patterns of calcined Bharatmoni catalysts.

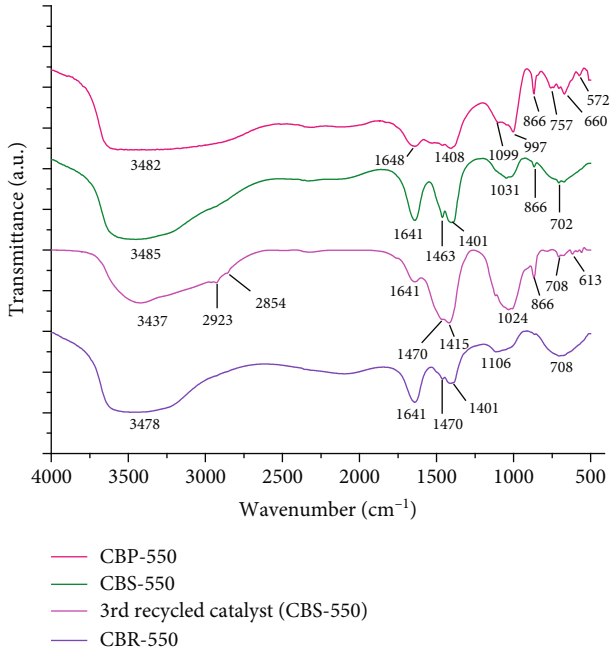

Figure 2: FT-IR spectra of calcined Bharatmoni catalysts.

The spectra exhibited for the catalyst CBP-550 at 1648 and 1408 cm^{-1}, CBS-550 (1641, 1463, and 1401 cm^{-1}), 3rd recycled catalyst (1641, 1470, and 1415 cm^{-1}), and CBR-550 at 1641, 1470, and 1401 cm^{-1} are representing the C-O stretching and bending vibrations that refer to the occurrence of carbonate (CO_3^{2-}) [17, 33]. The metal carbonate present in the catalyst also agreed with the XRD result (Figure 1). The peaks located at 1099, 997, and 866 cm^{-1} (CBP-550), 1031 and 866 cm^{-1} (CBS-550), 1024 and 866 cm^{-1} (recovered catalyst of CBS-550), and 1106 cm^{-1} (CBR-550) are due to Si-O-Si bond vibration [17, 47]. The bands at 757, 660, and 572 cm^{-1} (CBP-550), 702 cm^{-1} (CBS-550), 708 and 613 cm^{-1} (recovered catalyst), and 708 cm^{-1} (CBR-550) are indicative of Ca-O and K-O stretching bond vibrations [20, 33, 48]. Thus, this FT-IR study is supported by the results found in the XRD analyses (Figure 1).

3.1.3. BET Study. The BET surface areas of CBP-550, CBS-550, and CBR-550 catalysts were measured as 2.061, 0.730, and 0.857 $m^2 g^{-1}$. The measured pore volumes were 0.008, 0.002, and 0.002 $cm^3 g^{-1}$ for CBP-550, CBS-550, and CBR-550, respectively. Comparable surface areas were also reported in the catalysts prepared from some other biomasses such as peels of tucumã (1.0 $m^2 g^{-1}$) [49], straw slag (1.2 $m^2 g^{-1}$) [50], and activated wood ash (0.65$m^2 g^{-1}$) [51]. The method of preparation also influences the surface area, pore diameter, and pore volume values of the catalyst. Daimary et al. [27] reported the change in surface area, pore volume, and pore diameter values for the same catalyst (*Musa acuminata* peel) when prepared by two different methods. At high calcination temperatures, catalyst particles agglomerate leading to a low surface area [52]. According to the isotherm (Figure 3), the present catalysts showed type IV physisorption isotherms and demonstrated an H3 hysteresis loop. In this study, the obtained pore diameter of CBP-550, CBS-550, and CBR-550 catalysts were 4.059, 3.459, and 2.976 nm, respectively. The distribution of BJH pore size of CBP-550, CBS-550, and CBR-550 catalysts is found between the nanoparticle sizes of 2–50 nm confirming that the catalysts are mesoporous in nature. Eldiehy et al. [53] reported that waste sweet potato leaf-derived catalyst has a mesoporous structure illustrating physisorption isotherm type IV and H3 hysteresis loop. Similar results were reported by Oladipo et al. [44], Falowo and Betiku [54], and Betiku et al. [55], for the catalysts derived from the *Carica papaya* peel, agrowaste mixture, and kola nut husk, respectively. Although the present catalysts contained low surface areas, they have high catalytic activity which may be due to their porosity character and constituents of basic elements.

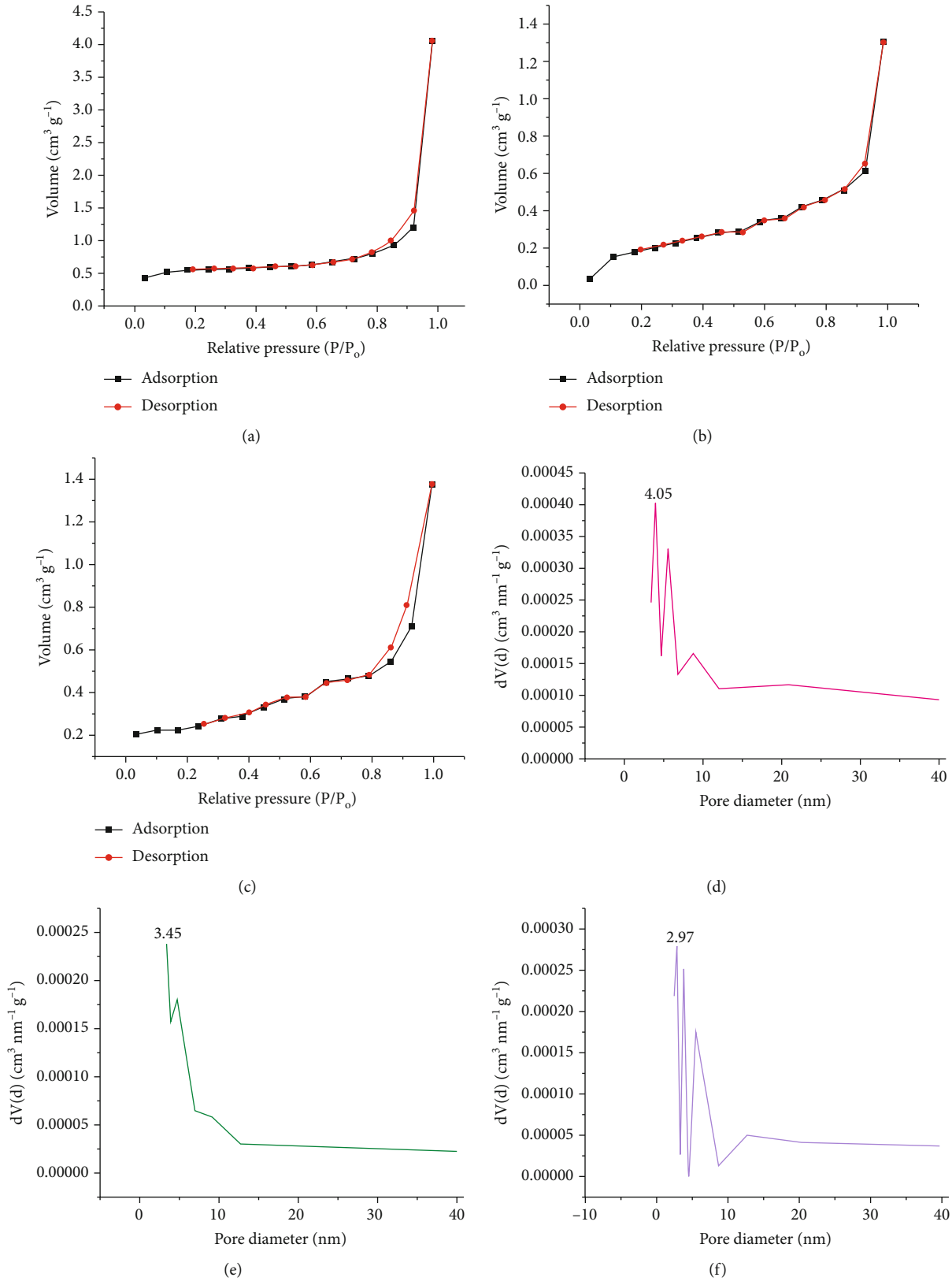

Figure 3: N_2 adsorption–desorption isotherms (a–c) and adsorption pore size distribution of CBP-550 (d), CBS-550 (e), and CBR-550 (f) catalysts.

3.1.4. FESEM and HR-TEM Analyses. The images analyzed by the FESEM technique are shown in Figure 4 (burnt ash material), Figure 5 (calcined catalysts), and Figure S2 (3rd recycled CBS-550 catalyst). It can be observed that the BBP catalyst exhibited a bead-like shape with holes indicating porosity features (Figure 4(a)). The BBS catalyst has

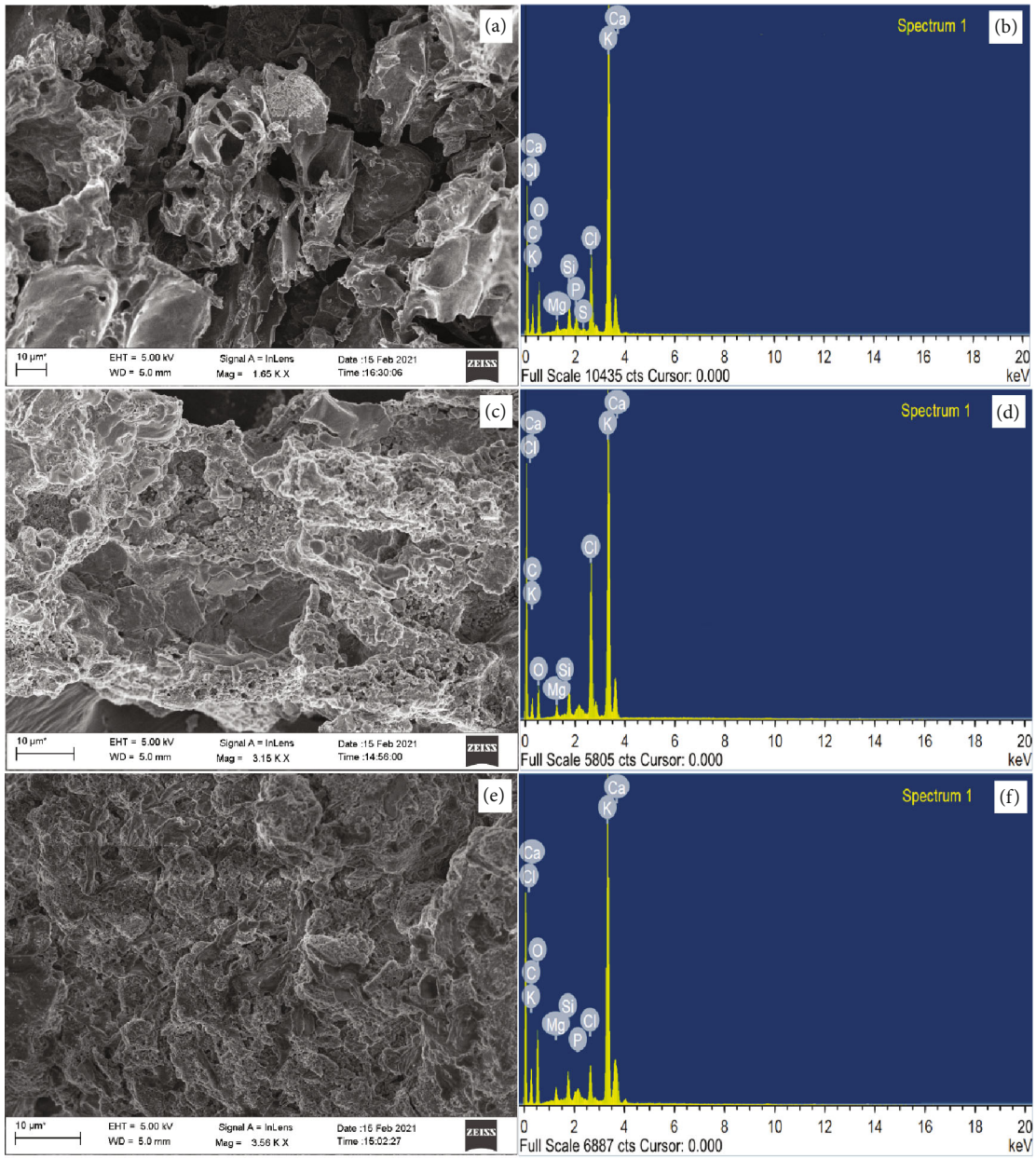

Figure 4: FESEM images (a, c, e) and EDX spectra (b, d, f) of BBP (a, b), BBS (c, d), and BBR (e, f) catalysts.

substances aggregated with mostly oval, polygons, and cylindrical shapes along with pores (Figure 4(c)). The analysis also demonstrated the porous nature of the BBR catalyst with compacted rough and aggregated particles (Figure 4(e)). The morphological difference in FESEM images can be observed in calcined catalysts (Figure 5) compared with burnt ash materials (Figure 4). The catalyst CBP-550 (Figure 5(a)) revealed the presence of more aggregated components with irregular spherical-like shapes having porous morphology. The surface morphological features of CBS-550 (Figure 5(c)) can be observed as rough clusters of tiny spheres and porous nature. The catalyst CBR-550 has no specific geometrical shapes, but it is a compact material with porous nature (Figure 5(e)). FESEM analysis of the recovered catalyst from the 3rd reaction cycled (Figure S2) showed that its outer morphology is shaped like a crushed cylindrical and oval as if some of the particles are washed out.

The HR-TEM images shown in Figure S3(A, B) are for the CBP-550 catalyst which displayed that it has aggregated particles with many nonuniform oval and spherical shapes and looks like porous particles. Figure S3(C, D) is the HR-TEM images of the CBS-550 catalyst that also revealed the porous materials and rough surface composed of tiny oval and polygon shapes. Similarly, the surface morphology of the CBR-550 catalyst recorded by the HR-TEM technique as shown in Figure S3(E, F) disclosed that the material is built up with compact particles without specific shapes and has

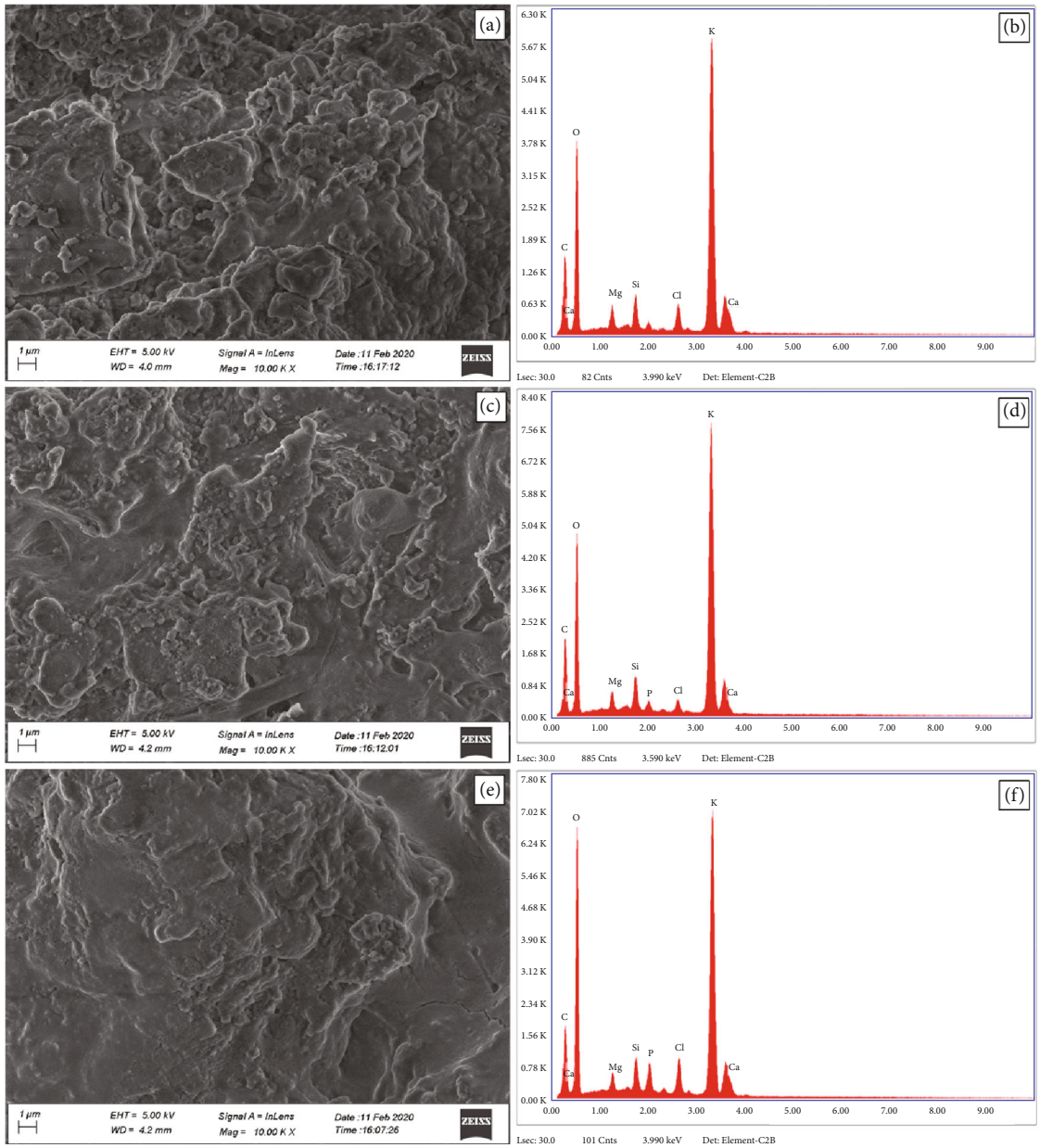

Figure 5: FESEM images (a, c, e) and EDX spectra (b, d, f) of CBP-550 (a, b), CBS-550 (c, d), and CBR-550 (e, f) catalysts.

some holes indicating its porous property. The existence of porosity of the present calcined catalysts also agreed with the BET study. The morphological results depicted in the FESEM study are supported by the results demonstrated in the HR-TEM studies.

3.1.5. EDX Analyses of the Catalysts. Tables 1 and 2 represent the analyzed elemental compositions of the derived catalysts. The obtained data explains that burnt ash and calcined catalysts of different parts of the Bharatmoni plant exhibit different elemental compositions. Figures 4(b), 4(d), and 4(f) illustrates the EDX patterns for BBP, BBS, and BBR catalysts that indicated the occurrence of K, C, O, Ca, Cl, Mg, and Si. Besides these, P is present in BBP and BBR and the S element is also found in BBP catalyst. Among the existing elements, K constituted the highest composition in the BBS (36.53%) catalyst (Table 1). The EDX patterns for CBP-550, CBS-550 and CBR-550 are represented in Figures 5(b), 5(d), and 5(f). After the burnt ash material was calcinated at 550°C, it revealed the increase of potassium composition with variable weight % and atomic % (Table 2). The CBP-550 catalyst consists of 44.88 wt% of K, CBS-550 catalyst showed 46.88 wt% of K, and CBR-550 catalyst exhibited K of 39.33 wt%. It is remarkable that among all the catalysts of this study, the CBS-550 catalyst has been observed with the highest quantity of potassium (Table 2). Since the CBS-550 catalyst has higher K content, it is expected to exhibit more K_2CO_3 and K_2O constituents as depicted in

Table 1: FESEM-EDX analyses of burnt Bharatmoni materials.

Elements	Composition of burnt Bharatmoni materials					
	BBP		BBS		BBR	
	Weight %	Atomic %	Weight %	Atomic %	Weight %	Atomic %
C	21.26	34.76	19.68	34.77	17.83	28.73
O	33.83	41.52	25.73	34.12	41.37	50.14
K	32.83	16.48	36.53	19.82	30.80	15.25
Ca	1.16	0.57	1.22	0.60	3.66	1.77
Mg	0.82	0.66	0.91	0.80	1.02	0.82
Si	1.81	1.26	2.15	1.63	1.91	1.32
P	1.70	1.08	—	—	0.48	0.30
Cl	6.42	3.55	13.75	8.22	2.87	1.57
S	0.18	0.11	—	—	—	—

Table 2: FESEM-EDX analyses of calcined Bharatmoni catalysts.

Elements	Composition of catalyst calcined at 550°C							
	CBP-550		CBS-550		3rd recycled catalyst (CBS-550)		CBR-550	
	Weight %	Atomic %	Weight %	Atomic %	Weight %	Atomic %	Weight %	Atomic %
C	4.67	8.92	6.46	12.15	24.63	35.79	4.55	8.36
O	39.86	57.17	38.96	55.00	45.29	49.41	44.52	61.39
K	44.88	26.34	46.88	27.08	13.06	5.82	39.33	22.19
Ca	3.40	1.95	1.15	0.65	8.18	3.56	2.01	1.11
Mg	1.92	1.81	1.53	1.42	2.29	1.65	1.45	1.32
Si	2.28	1.86	2.49	2.01	3.50	2.17	2.16	1.70
P	—	—	1.00	0.73	1.76	0.99	2.42	1.73
Cl	3.00	1.94	1.52	0.97	1.06	0.52	3.55	2.21
Mn	—	—	—	—	0.19	0.06	—	—

analyses of FT-IR (Figure 2) and XRD (Figure 1), and that may be a reason for showing the highest catalytic activity. Etim et al. [21], Gohain et al. [33], and Tarigan et al. [45] have also found high K in their catalysts prepared from biomass sources and reported good catalytic activities. In Table 3, the composition of the elements of the CBS-550 catalyst is compared with other catalysts reported from different biomass sources. From the comparison, it can be understood that the present catalyst (CBS-550) has a higher K concentration showing better catalytic activity than other catalysts mentioned in Table 3. As the catalyst CBS-550 showed the best activity with high K, it was tested for reusability up to the 3rd cycle and the examined EDX for 3rd recycled catalyst is depicted in Figure S2D and its elemental compositions are shown in Table 2. It is seen that the K concentration in 3rd recycled catalyst has reduced, resulting in reduced catalytic activity due to its decrease in basic site elements. The recycled catalysts of orange peel ash and *Musa champa* peduncle studied by Changmai et al. [56] and Nath et al. [57], respectively, have also reported the comparable EDX analyzed data with the reduction of active components after being employed in the transesterification reaction.

3.1.6. XPS Study. XPS analysis results of burnt ash materials (BBP, BBS, and BBR), calcined catalysts (CBP-550, CBS-550, and CBR-550) and regenerated catalyst from the 3rd reaction cycle are shown in Figures 6 and 7. The determined surface elemental compositions are summarized in Table 4. The existence of O, C, and K elements are found mainly with high concentration (atomic %) along with Ca, Mg, Fe, Mn, Si, Zn, and Sr. The deconvoluted spectrum (Figure 6(b)) of C 1s for BBP was noticed at the binding energies of 284.89 and 288.55 eV. The binding energies are observed at 284.86 eV and 288.58 eV for BBS and at 284.81 eV and 288.56 eV for BBR (Figure 6(b)). On the other hand, for calcined catalysts, the presence of C 1s is denoted in Figure 7(b) at two different binding energies of 284.81 and 288.60 eV for CBP-550, 284.70 and 288.32 eV for CBS-550, and 284.68 and 288.22 eV for CBR-550 and observed at 284.81 and 284.08 eV for the recovered catalyst. These peaks revealed in XPS spectra for every catalyst signify the occurrence of C=O and C-C bonds that support the presence of metal carbonates [26]. The XPS spectra for O 1s (Figures 6(c) and 7(c)) revealed binding energies of 530.82 eV (BBP), 530.75 eV (BBS), 530.98 eV (BBR), 530.71 eV (CBP-550), 530.60 eV (CBS-550), 530.56 eV (CBR-550), and 531.37 eV (recovered catalyst), indicating the presence of oxygen occurring as metal

Table 3: Elemental composition of Bharatmoni catalyst and its comparison with other reported solid catalysts derived from waste biomasses.

Source of catalyst	Calcination condition	Composition (%)							
		K	Ca	Mg	Si	P	Cl	C	O
Bharatmoni stem (this work)	550°C, 2 h	46.88	1.15	1.53	2.49	1.00	1.52	6.46	38.96
Passion fruit peel [45]	400°C, 4 h	44.4					16.6	7.9	
Citrus sinensis peel [56]	Burnt	8.95	5.01	1.30	—	—	—	—	37.20
Carica papaya peel [21]	700°C, 4 h	36.74	3.64	1.16	0.71	4.22	10.3	—	44.1
Musa balbisiana peel [33]	700°C, 4 h	41.37	36.08	12.02	—	—	—	—	—
Musa acuminata peduncle [31]	Uncalcined	25.63	—	0.97	0.56	0.78	—	—	72.06
Heteropanax fragrans [79]	550°C, 2 h	19.05	5.13	0.86	8.51	0.64	1.92	16.71	46.74
Camphor leaf [85]	800°C, 2 h	1.22	12.05	1.82	—	—	—	—	—
Musa acuminata peduncle [31]	700°C, 4 h	42.23	1.70	1.39	1.54	1.91	—	—	50.54
Poovan banana pseudostem [24]	700°C, 4 h	20.2	7.4	4.52	3.79	1.91	8.99	—	—
Lemna perpusilla [23]	550°C, 2 h	11.32	—	—	82.51	—	—	5.10	—
Pawpaw peel [44]	600°C, 4 h	23.89	2.86	1.00	0.00	3.04	0.87	29.16	36.72
Musa balbisiana underground stem [75]	550°C, 2 h	25.09 (K_2O)	10.44 (CaO)	10.04 (MgO)	35.92 (SiO_2)	4.47 (P_2O_5)	—	—	—
Acacia nilotica stem [51]	800°C	5.7	17.8	4.5	21.5	0.5	—	—	—
Acacia nilotica stem [51]	500°C	6.7	13.3	2.7	15.7	0.80	—	—	—
Moringa leaves [78]	500°C, 2 h	9.87	10.09	5.92	—	1.19	—	12.19	59.57
Snail shell [77]	900°C, 4 h	—	68.8	0.1	0.3	0.00	—	4.6	26.1
Sesamum indicum [2]	550°C, 2 h	29.64	33.80	9.68	11.32	—	—	—	—
Sugarcane bagasse [60]	550°C, 2 h	12.07	2.43	1.12	24.11	2.14	—	5.89	50.22

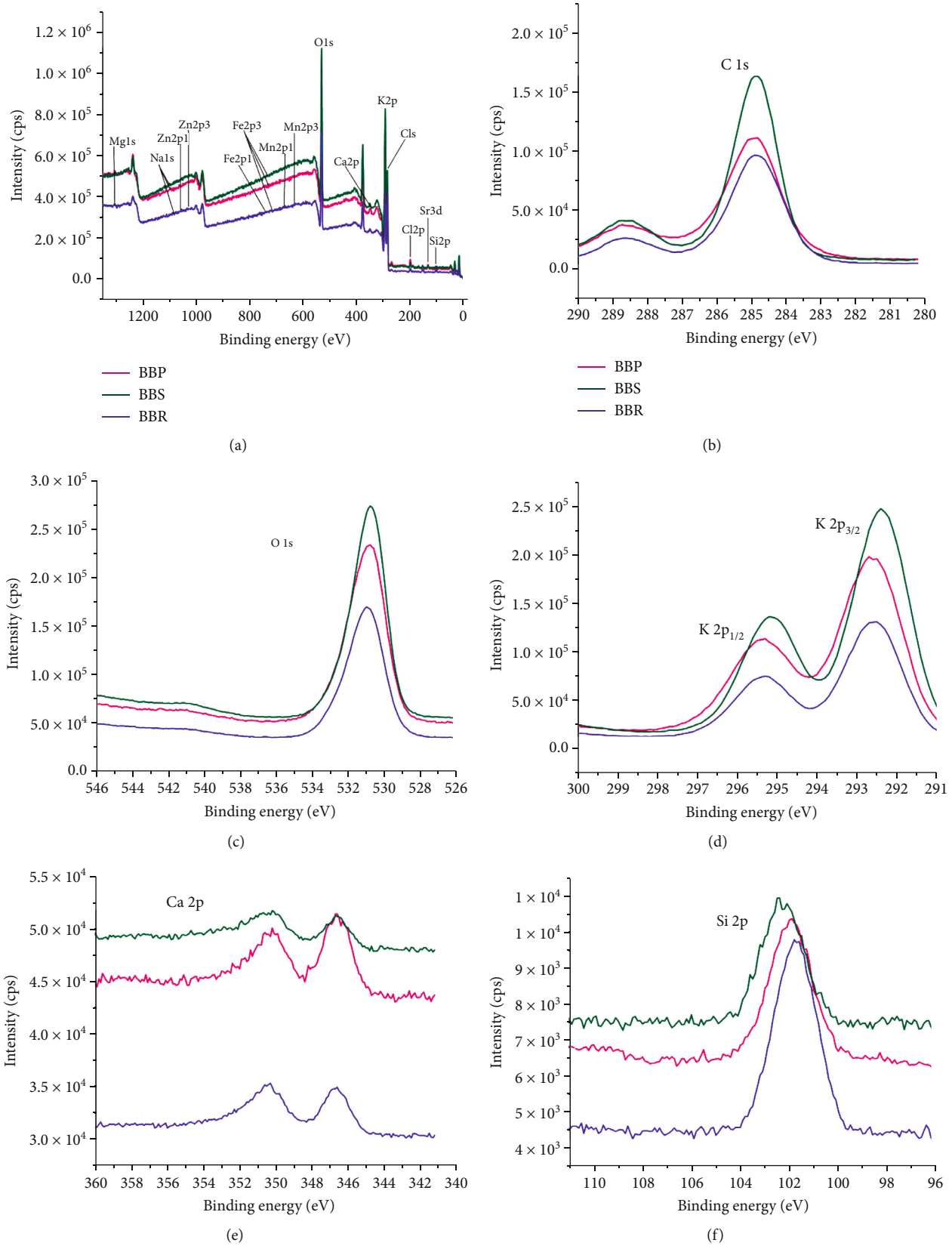

Figure 6: XPS survey spectra (a) of BBP, BBS, and BBR catalysts; XPS patterns of C 1s (b), O 1s (c), K 2p (d), Ca 2p (e), and Si 2p (f).

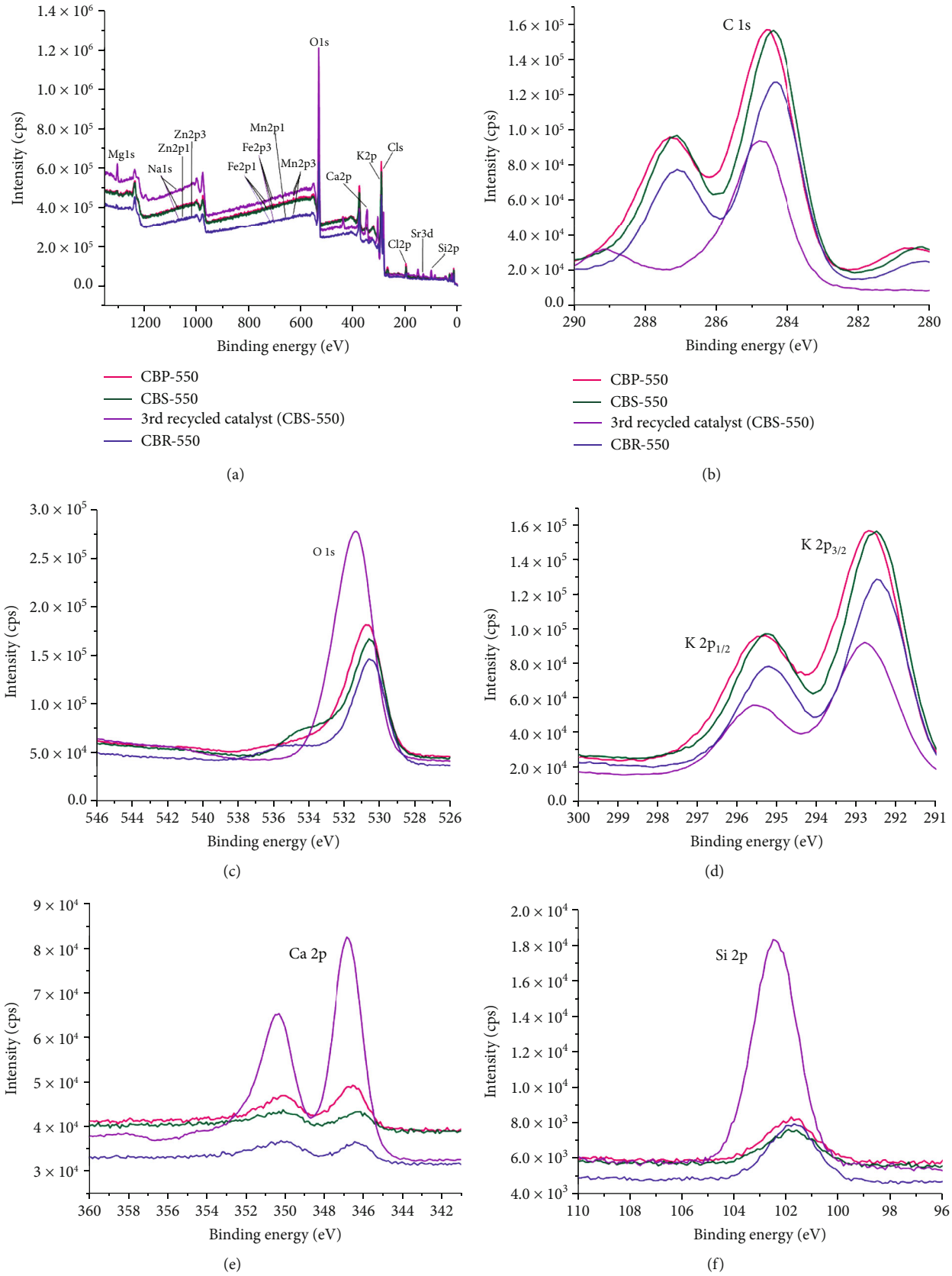

Figure 7: XPS survey spectra (a) of CBP-550, CBS-550, CBR-550, and 3rd recycled catalysts; XPS patterns of C 1s (b), O 1s (c), K 2p (d), Ca 2p (e), and Si 2p (f).

Table 4: XPS analyses of burnt and calcined Bharatmoni catalysts.

Elements	Composition of burnt Bharatmoni materials			Composition of catalyst calcined at 550°C			
	BBP Atomic %	BBS Atomic %	BBR Atomic %	CBP-550 Atomic %	CBS-550 Atomic %	3rd recycled catalyst (CBS-550) Atomic %	CBR-550 Atomic %
O 1s	24.91	23.05	36.1	19.38	21.26	50.26	20.59
C 1s	58.2	60.36	46.97	51.72	50.72	27.42	50.48
K 2p	11.41	11.48	10.23	18.45	19.44	5.81	17.57
Ca 2p	0.79	0.33	0.05	0.23	0.09	5.41	0.11
N 1s	—	2.39	—	—	—	—	—
Na 1s	—	—	—	0.12	0.08	0.09	0.38
Mg 1s	0.31	0.12	0.18	0.06	0.25	2.55	0.13
Mn 2p	0.49	0.09	0.35	0.34	0.28	0.34	0.14
Fe 2p	0.26	0.38	0.86	0.24	0.4	0.33	0.42
Zn 2p	0.05	0.18	0.37	0.17	0.33	0.51	0.44
Si 2p	1.45	—	3.3	6.13	4.17	5.42	7.43
Sr 3d	0.98	0.4	0.35	0.27	0.63	1.26	0.66
Cl 2p	1.15	0.63	1.03	2.9	2.33	0.61	1.65

oxides and carbonates [53]. Figures 6(d)7(d) illustrate two peaks for K 2p at the binding energies of 292.66 and 295.31 eV (BBP), 292.37 and 295.18 eV (BBS), 292.57 and 295.35 eV (BBR), 292.69 eV and 295.32 eV (CBP-550), 292.49 and 295.24 eV (CBS-550), 292.48 and 295.22 eV (CBR-550), and 292.78 and 295.54 eV (3rd recycled catalyst). Out of the appeared two distinct peaks for each catalyst, the lower binding energy ascribed to K $2p_{3/2}$ and the peak at higher binding energy correspond to K $2p_{1/2}$ which demonstrated the existence of K as +1 state in the form of K_2O and K_2CO_3 in all the catalysts of this work [57]. The two hump peaks appeared (Figures 6(e) and 7(e)) for Ca 2p with the binding energies of 346.63 and 350.18 eV (BBP), 346.65 and 350.14 eV (BBS), 346.67 and 350.30 eV (BBR), 346.58 and 350.17 eV (CBP-550), 346.49 and 350.30 eV (CBR-550), and 346.77 and 350.32 eV (recovered catalyst) established the occurrence of Ca oxide or carbonate in the present catalysts [58]. The Si 2p spectra (Figures 6(f) and 7(f)) revealed a single peak at a lower binding energy of 101.88 eV (BBP), 102.42 eV (BBS), 101.79 eV (BBR), 101.83 eV (CBP-550), 101.71 eV (CBS-550), 101.67 eV (CBR-550), and 102.47 eV for the recovered catalyst, and this is due to Si-O bond [59]. The XPS studies of the present catalysts concluded that the calcined catalysts exhibited more concentrations of O, C, and K (Table 4) compared to the burnt ash materials. The investigated XPS data showed the occurrence of K as one of the dominant elements existing as K_2O and K_2CO_3 in the calcined catalysts, which is mainly responsible for the base catalysis of this study. These data also coincided with the results of the EDX (Table 2) investigations.

3.1.7. Determination of pH Values. The measured pH values of the present calcined catalysts are depicted in Figure 8. In the ratio from 1 : 5 to 1 : 40 of catalyst weight by volume of distilled water (*w*/*v*), CBS-550 catalyst showed a higher pH value indicating highly basic. The root cause of the high basic character of the CBS-550 catalyst is possibly

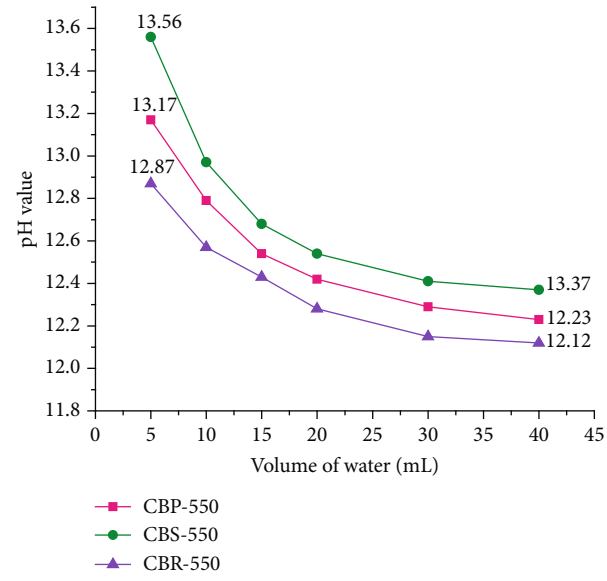

Figure 8: Variation of pH values of calcined Bharatmoni catalysts (1 g) dissolved with different volumes of water.

due to the existence of higher compositions of potassium existing in the form of K_2CO_3 and K_2O as the basic active species. The high constituents of potassium, oxygen, and carbon in the CBS-550 catalyst were supported by the analysis results of EDX technique (Table 2) and XPS (Table 4). It is also found that the CBS-550 catalyst containing a high pH value showed the superior catalytic activity in this study. In other studies, the reported pH value of the base catalysts prepared from biomasses like sugarcane bagasse (pH = 12.10 at 1 : 5 *w*/*v*) [60], *Sesamum indicum* (pH = 11.4 at 1 : 10 w/v) [2], and *Brassica nigra* (pH = 11.91 at 1 : 5 *w*/*v*) [19] exhibited lower pH values than the current calcined catalysts.

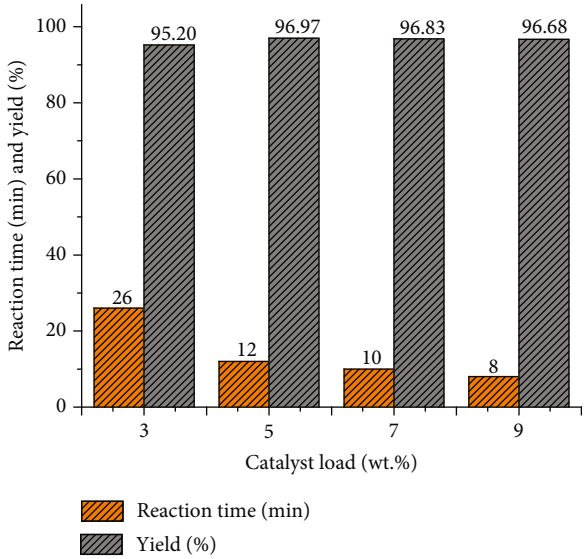

Figure 9: Effect of catalyst loading of calcined Bharatmoni stem (CBS-550) on biodiesel synthesis (temperature = 65°C, MTOMR = 9 : 1).

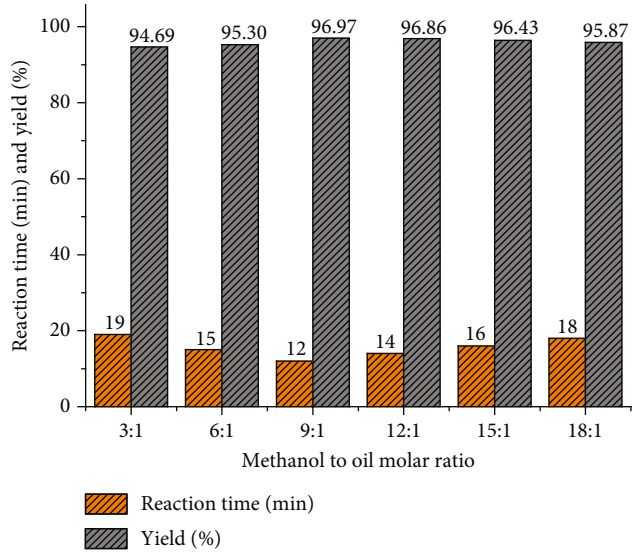

Figure 10: Effect of MTOMR on biodiesel synthesis (temperature = 65°C, CBS-550 catalyst = 5 wt%).

3.1.8. Soluble Alkalinity, Basicity, and Turnover Frequency (TOF) Studies. The determined values of soluble alkalinity of CBP-550, CBS-550, and CBR-550 were 5.31, 5.54, and 4.97 mmol g^{-1}, respectively. It can be noticed that a higher soluble alkalinity value was found in the CBS-550 catalyst. The reason for higher soluble alkalinity may be due to the presence of an enormous amount of K and Ca in carbonate form which is supported by the analyses of FT-IR and XRD [49, 51]. Sharma et al. [51] also tested soluble alkalinity and reported a higher value of 12.7 mmol g^{-1} for wood-based ash material showing good catalytic activity. The lower soluble alkalinity values were found by Mendonça et al. [49], Mendonça et al. [61], and Barros et al. [62] for the catalysts prepared from peels of tucumã (3.71 mmol g^{-1}), cupuaçu (1.05 mmol g^{-1}), and pineapple leaves (0.39 mmol g^{-1}), respectively.

From the Hammett test, the basicity of CBP-550, CBS-550, and CBR-550 catalysts was measured as 1.36, 1.45, and 1.26 mmol g^{-1}, respectively. The present Bharatmoni catalysts revealed the basic strength within the range 10.1 < H_< 18.4. CBS-550 catalyst has the highest basicity and is because of the higher concentration of K constituted as carbonate and oxide along with other basic components like CaO and $CaCO_3$ [27]. The abundance of basic sites is evident by the results of XPS, EDX, and XRD analyses of this study. The lower basicity values were reported for sugarcane bagasse (0.0891 mmol g^{-1}) [60], barium cerate (1.74 mmol g^{-1}) [63], and *Citrus sinensis* peel (0.170 mmol g^{-1}) [56] catalysts which were also employed in the synthesis of biodiesel.

Based on the basicity values determined, the catalytic efficiencies concerning turnover frequency (TOF) of CBP-550, CBS-550, and CBR-550 catalysts were calculated [41]. TOF measures the efficiency of a catalyst, which is one of the main parameters for commercial or industrial catalysts and describes how many biodiesel molecules can be produced per unit of the basic active site and per unit of time [64]. The calculated TOF values of CBP-550, CBS-550, and CBR-550 catalysts were 7.98 h^{-1}, 10.03 h^{-1}, and 7.66 h^{-1}, respectively. The comparable TOF values were reported in *Musa chinensis* peel (16.85 h^{-1}) and trunk (7.025 h^{-1}) catalysts [58] and sugarcane bagasse catalyst (6.59 h^{-1}) [60]. Roy et al. [64] reported a lower TOF value of 4.29 h^{-1} for the K-based lanthanum oxide employed as the catalyst in the biodiesel synthesis.

4. Role of Bharatmoni Catalysts in the Biodiesel Synthesis

4.1. Effect of Catalyst Concentration. In this study, the CBS-550 catalyst loaded based on the *J. curcas* oil's weight in the reaction mixture of 9 : 1 MTOMR (methanol-to-oil molar ratio) and the reaction set up at 65°C was investigated. The amount of catalyst loaded in the reaction is a significant parameter to attain the optimized condition for the production of biodiesel. The reactions loaded with 3, 5, 7, and 9 wt% of the CBS-550 catalyst and its outcome with different biodiesel yields (%) produced at varying time periods are illustrated in Figure 9. The reaction catalyzed by adding 3 and 5 wt% of catalyst completed with a reduced reaction time from 26 min to 12 min with increasing biodiesel yield from 95.20% to 96.97%, respectively (Figure 9). The reason for reducing reaction time and increasing yield (%) with loading more catalyst is due to more abundance of basic active sites [17]. The biodiesel yield (%) is maximum in reaction loaded with 5 wt% catalyst. The reaction loaded with 7 and 9 wt% of the catalyst produced lower biodiesel yield (Figure 9). This is because the reaction with a higher amount of catalyst may worsen the mass transfer between the unmixable reactants by making the mixture more viscous leading to the hindrance of diffusion [65]. Pathak et al. [20], Oladipo et al. [44], and Falowo and Betiku [54] also reported from their studies that the biodiesel yield rises to a certain optimum

Table 5: Rate constant (k), correlation coefficient (R^2), activation energy (E_a), and pre-exponential factor (A) of various kinetic models of the reaction catalyzed by CBP-550 catalyst.

Order of reaction	Rate constant, k (s^{-1}) at various temperature (K)					R^2 value	Activation energy, E_a ($kJ\,mol^{-1}$)	Pre-exponential factor, A (s^{-1})
	308	318	328	338	348			
Zero order	9.05×10^{-6}	1.57×10^{-5}	2.68×10^{-5}	3.24×10^{-5}	3.89×10^{-5}	0.93699	32.75	3.65
First order	9.31×10^{-6}	1.60×10^{-5}	2.74×10^{-5}	3.29×10^{-5}	3.96×10^{-5}	0.93652	32.49	3.39
Pseudo-first order	4.86×10^{-4}	1.14×10^{-3}	2.04×10^{-3}	3.62×10^{-3}	4.07×10^{-3}	0.94786	48.56	9.82×10^{4}
Second order	1.03×10^{-6}	1.78×10^{-6}	3.04×10^{-6}	3.66×10^{-6}	4.40×10^{-6}	0.93646	32.46	3.73×10^{-1}

Table 6: Rate constant (k), correlation coefficient (R^2), activation energy (E_a), and pre-exponential factor (A) of various kinetic models of the reaction catalyzed by CBS-550 catalyst.

Order of reaction	Rate constant, k (s^{-1}) at various temperature (K)					R^2 value	Activation energy, E_a ($kJ\,mol^{-1}$)	Pre-exponential factor, A (s^{-1})
	308	318	328	338	348			
Zero order	1.09×10^{-5}	2.28×10^{-5}	3.07×10^{-5}	4.21×10^{-5}	5.20×10^{-5}	0.93721	33.47	6.11
First order	1.12×10^{-6}	2.33×10^{-5}	3.13×10^{-5}	4.27×10^{-5}	5.28×10^{-5}	0.93673	33.31	5.88×10^{4}
Pseudo-first order	8.09×10^{-4}	1.77×10^{-3}	3.15×10^{-3}	4.86×10^{-3}	5.78×10^{-3}	0.95033	44.36	3.16×10^{4}
Second order	1.25×10^{-6}	2.60×10^{-6}	3.48×10^{-6}	4.76×10^{-6}	5.88×10^{-6}	0.93667	33.30	6.50×10^{-1}

Table 7: Rate constant (k), correlation coefficient (R^2), activation energy (E_a), and pre-exponential factor (A) of various kinetic models of the reaction catalyzed by CBR-550 catalyst.

Order of reaction	Rate constant, k (s^{-1}) at various temperature (K)					R^2 value	Activation energy, E_a ($kJ\,mol^{-1}$)	Pre-exponential factor, A (s^{-1})
	308	318	328	338	348			
Zero order	8.51×10^{-6}	1.66×10^{-5}	1.94×10^{-5}	3.21×10^{-5}	3.89×10^{-5}	0.95274	33.11	3.89
First order	8.77×10^{-6}	1.70×10^{-5}	1.99×10^{-5}	3.27×10^{-5}	3.96×10^{-5}	0.95201	32.81	3.58
Pseudo-first order	4.11×10^{-4}	8.81×10^{-4}	1.37×10^{-3}	3.11×10^{-3}	3.43×10^{-3}	0.95766	49.26	1.01×10^{5}
Second order	9.78×10^{-7}	1.90×10^{-6}	2.21×10^{-6}	3.64×10^{-6}	4.41×10^{-6}	0.95192	32.78	3.94×10^{-1}

amount of catalyst load and it was known to drop with excessive catalyst load. Thus, the optimal catalyst dose for the present transesterification reaction is 5 wt%.

4.2. Effect of MTOMR. MTOMR is one of the important factors that influence the biodiesel yield and reaction time of the reaction. Stoichiometrically, in a transesterification reaction, 3 : 1 MTOMR is required to synthesize 3 moles of methyl esters and one mole of glycerol. In this study, adding different MTOMRs ranging from 3 : 1 to 18 : 1 in the reaction using 5 wt% of CBS-550 catalyst at 65°C was investigated to obtain the optimum MTOMR and the results are represented in Figure 10. When MTOMR was increased from 3 : 1 to 9 : 1, it was observed that the biodiesel yield increases from 94.69% to 96.97% along with a gradual reduction of reaction time from 19 min to 12 min. It can be explained that a larger volume of methanol than the required stoichiometric ratio can speed up the transesterification reaction. The excess methanol forms methoxy species on the surface of the catalyst which is essential to drive the reaction in the forward direction to maintain the equilibrium since the transesterification reaction is reversible [66]. Using MTOMR from 12 : 1 to 18 : 1, the biodiesel yield decreased from 96.86% to 95.87% with an increase in reaction time from 14 to 18 min (Figure 10). The observed effect at large MTOMR is due to the fact that the reaction system gets diluted with excessive methanol and the catalyst's active sites on the surface get hampered which reduces the interaction between the triglyceride and catalyst and thus prevents the conversion of biodiesel. Furthermore, excessive methanol dissolves the byproduct glycerol which makes it difficult and lengthy to separate from biodiesel [65, 67]. Therefore, the optimum MTOMR determined for this work is 9 : 1.

4.3. Effect of Temperature. One of the most significant parameters that affect the transesterification is the temperature. In this study, the effect of temperature was investigated under the MTOMR of 9 : 1 and 5 wt% of catalyst by utilizing the three calcined catalysts (CBP-550, CBS-550, and CBR-550). The experimental results are represented in Figure S4. The experiments revealed that with rising temperatures from 35°C to 75°C, the reaction time decreased. The improvement in the yield of

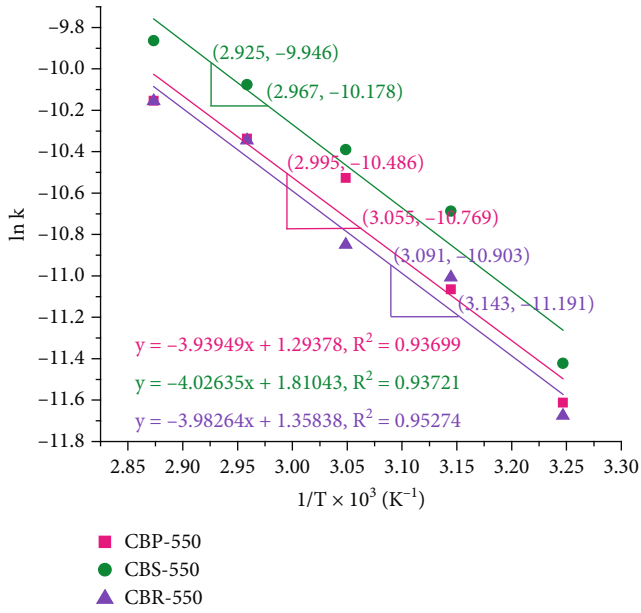

Figure 11: The Arrhenius plot (ln k versus $1/T \times 10^3$) for the reaction of zero-order rate model employing Bharatmoni catalysts (reaction temperatures = 35, 45, 55, 65, and 75°C).

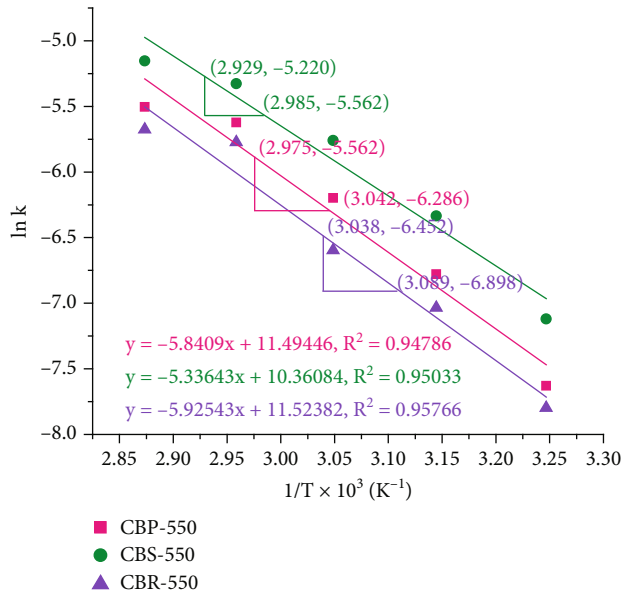

Figure 12: The Arrhenius plot (ln k versus $1/T \times 10^3$) for the reaction of pseudo-first-order rate model employing Bharatmoni catalysts (reaction temperatures = 35, 45, 55, 65, and 75°C).

biodiesel was noticed till the reaction temperature of 65°C. All the examined reactions at 75°C catalyzed by the three calcined catalysts showed no substantial improvement in biodiesel yield because methanol evaporates at 75°C that possibly leads to the less interaction of the reaction mixture [56, 68]. Hence, the transesterification reaction at 65°C catalyzed by the calcined catalysts showed the highest biodiesel yield in the order of CBS-550 (96.97% in 12 min) > CBP-550 (96.89% in 16 min) > CBR-550 (96.53% in 18 min) (Figure S4). The

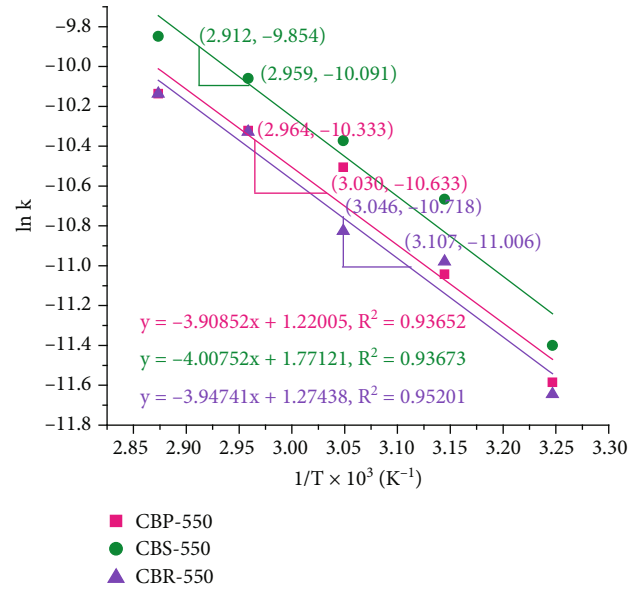

Figure 13: The Arrhenius plot (ln k versus $1/T \times 10^3$) for the reaction of first-order rate model employing Bharatmoni catalysts (reaction temperatures = 35, 45, 55, 65, and 75°C).

efficiency of CBS-550 catalyst was found to be higher which agreed with the trends of higher potassium concentration (Table 2) and basic sites of the catalysts. The burnt ashes were also utilized to examine their activities at 65°C and found that the BBS catalyst had yielded maximum biodiesel of 96.67% in 25 min followed by BBP (96.19% in 30 min) and BBR (95.73% in 45 min) (Figure S5). Among the burnt ash materials, the BBS catalyst showed higher catalytic activity that follows the trends of potassium concentration (Table 1). In this study, the reaction at 65°C resulted in a maximum yield of 96.97% within a short duration, and hence, this temperature is considered to be optimum.

4.4. Reusability of Bharatmoni Catalyst. In this work, the reusability tests of the catalyst have been performed by utilizing the CBS-550 catalyst employing the optimum reaction parameters of 9 : 1 MTOMR and 5 wt% catalyst amounts at 65°C. A filtration process was carried out by using a suction pump to regenerate the fresh used catalyst from initial (first) reaction. It was then washed with petroleum ether 3-4 times to remove all the adhered substances (glycerol and methyl esters) from the catalyst. Thereafter, the recovered catalyst was taken in a petri dish to dry at 110°C for 4 h in a hot air oven; following that, the catalyst was allowed to cool under a desiccator and reused for subsequent reactions up to 3rd cycle following a similar reaction and the catalyst separation procedures. It has been that the CBS-550 catalyst is effectively reusable up to the 3rd cycle revealing the reduction in catalytic activity and biodiesel yield after every subsequent cycle (Figure S6). It is observed that the regenerated catalyst produced biodiesel of 95.67% in 45 min (1st cycle), 94.43% in 105 min (2nd cycle), and 93.20% in 150 min (3rd cycle). This decline in catalytic activity is due to the leaching of active elements [45]. The catalyst sample regenerated after 3rd cycle was analyzed by FT-IR

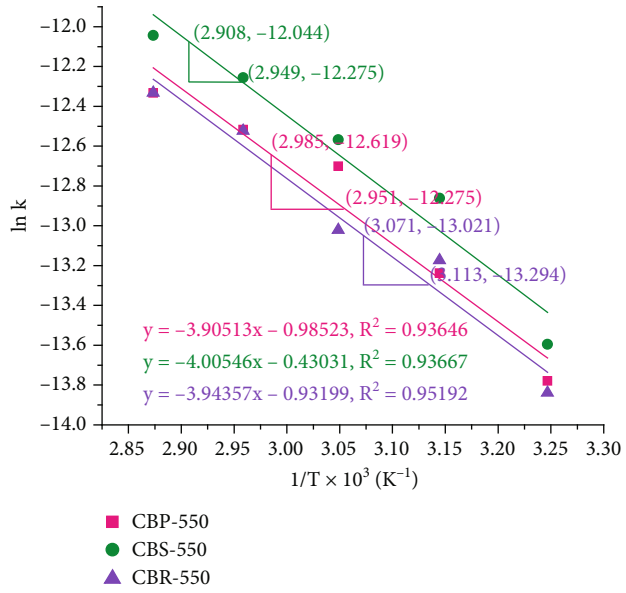

Figure 14: The Arrhenius plot (ln k versus $1/T \times 10^3$) for the reaction of second-order rate model employing Bharatmoni catalysts (reaction temperatures = 35, 45, 55, 65, and 75°C).

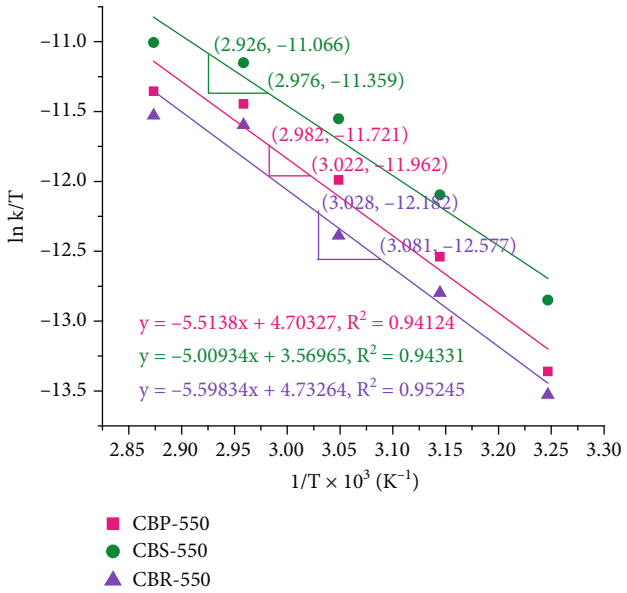

Figure 15: The Eyring–Polanyi plot (ln k/T versus $1/T \times 10^3$) for the study of thermodynamic properties of the reaction employing the Bharatmoni catalysts.

(Figure 2), FESEM-EDX (Figure S2), and XPS technique (Table 4). The FT-IR analysis revealed two new weak peaks at 2923 and 2854 cm^{-1} which are assigned to the C-H bond stretching indicating the contamination of the catalyst probably with glycerol or ester molecules, and it causes the blockage of pores of the catalyst resulting in a declined catalytic activity [27]. The morphological differences were noticed between the fresh catalyst sample (CBS-550) and the 3rd recycled catalyst (Figure 5 and Figure S2). The 3rd recycled catalyst has crushed cylindrical and oval shapes having its components washed out as compared to the structure of the fresh catalyst that has more aggregated components. EDX study revealed that 3rd recycled catalyst has a lower K concentration than the fresh CBS-550 catalyst (Table 2). The lowering of K concentration in the recovered catalyst was also detected in the XPS study (Table 4), which was primarily caused by the leaching out of the active components when the catalyst was reutilized for the 3rd reaction cycle [69].

4.5. Kinetic Study. Basically, the complete scheme of the reaction of triglyceride (TG) with methanol (CH_3OH) catalyzed by heterogeneous base catalyst occurs via three consecutive steps as shown in equations (3)–(5). During each intermediate step, 1 mole of methanol reacts with 1 mole of the glyceride compound to produce 1 mole of biodiesel (FAME). At the end of the reaction, three moles of FAME and one mole of glycerol are produced from 1 mole of TG. Thus, the reaction can be summarized as shown in equation (6) [57, 70].

$$\text{Triglyceride (TG)} + CH_3OH \rightleftharpoons \text{FAME} + \text{diglyceride (DG)} \quad (3)$$

$$\text{Diglyceride (DG)} + CH_3OH \rightleftharpoons \text{FAME} + \text{monoglyceride (MG)} \quad (4)$$

$$\text{Monoglyceride (MG)} + CH_3OH \rightleftharpoons \text{FAME} + \text{glycerol (GL)} \quad (5)$$

$$\text{Triglyceride (TG)} + 3\,CH_3OH \rightleftharpoons 3\,\text{FAME} + \text{glycerol (GL)} \quad (6)$$

In this work, kinetic studies of reactions for biodiesel production catalyzed by CBP-550, CBS-550, and CBR-550 catalysts were investigated. The reaction kinetics were determined with data achieved from the reactions performed under the optimized parameters, i.e., loaded with 5 wt% of catalyst and MTOMR of 9 : 1 at the reaction temperatures ranging from 35 to 75°C (Figure S4). Initially, the rate constants (k) were determined by substituting the required data in the following standard kinetic equations [57].

$$\text{Zero-order reaction, } k = \frac{[\text{TG}]_o - [\text{FAME}]}{t},$$

$$\text{First-order reaction, } k = \frac{2.303}{t} \log \frac{[\text{TG}]_o}{[\text{FAME}]},$$

$$\text{Pseudo-first-order reaction, } k = -\frac{2.303}{t} \log (1 - [\text{FAME}]),$$

$$\text{Second-order reaction, } k = \frac{1}{t} \times \frac{2.303}{([\text{TG}]_o - a)} \log \frac{a([\text{TG}]_o - x)}{[\text{TG}]_o(a - x)}, \quad (7)$$

where [FAME] is the concentration of the produced biodiesel at a time "t," $[\text{TG}]_o$ is the initial concentration

Table 8: Thermodynamic properties of the reaction catalyzed by CBP-550, CBS-550, and CBR-550 catalysts.

Catalysts	Thermodynamic properties						
	ΔH (kJ mol^{-1} K^{-1})	ΔS (kJ mol^{-1} K^{-1})	ΔG (kJ mol^{-1})				
			308 K	318 K	328 K	338 K	348 K
CBP-550	45.84	-1.039	727.45	376.25	386.64	397.03	407.42
CBS-550	41.64	-1.048	364.57	375.05	385.54	396.02	406.51
CBR-550	46.54	-1.038	366.49	376.88	387.26	397.65	408.04

of *J. curcas* oil, "a" is the initial concentration of methanol which is 9 (based on optimum MTOMR = 9 : 1), and "x" is the difference of $[TG]_o$ and [FAME] at a time "t."

The rate constants for various kinetic order reactions determined at various temperatures (in Kelvin, K) for the transesterification catalyzed by CBP-550, CBS-550, and CBR-550 catalysts are presented in Tables 5–7. Using these data, Arrhenius plots for different orders of reactions are derived and can be visualized in Figures 11–14. All the Arrhenius plots were linearly fitted to provide lines which was straight and the resultant correlation coefficients (R^2 value) as shown in Tables 5–7. As a consequence of the linear graphs of all the reaction models, the one which is the best fit with the highest correlation coefficient value was selected to determine the specific reaction order [70]. By employing the CBR-550 catalyst, the reaction had the highest R^2 value of 0.95766 (Table 7) followed by the CBS-550 catalyst (R^2 value = 0.95033, Table 6), and CBP-550 catalyst (R^2 value = 0.94786, Table 5) and all of these belonged to the model of pseudo-first-order reaction. Hence, it can be concluded that the current biodiesel production reaction catalyzed by the calcined Bharatmoni catalysts (CBP-550, CBS-550, and CBR-550) is following the kinetic model of pseudo-first-order reaction. These results were found similar in the works of Kaur et al. [71], Farid et al. [72], Yahya et al. [70], and Nath et al. [57] and reported that the synthesis of biodiesel with addition of excessive of methanol followed the pseudo-first-order kinetics.

The activation energies (E_a) were calculated by applying the slope = E_a/R obtained from the respective Arrhenius plots (Figures 11–14) ($R = 8.314\,\text{J K}^{-1}\,\text{mol}^{-1}$), and the pre-exponential factor (A) values were also evaluated from the intercept (ln A) of the plots (Figures 11–14). The calculated E_a and A values can be seen in Tables 5–7. Based on the kinetic model of pseudo-first order, the reaction catalyzed by the CBS-550 catalyst has the lowest E_a value (44.36 kJ mol^{-1}) than CBP-550 (48.56 kJ mol^{-1}) and CBR-550 (49.26 kJ mol^{-1}) catalysts. This result supports that the CBS-550 catalyst has the highest catalytic activity among the other two catalysts of this study (CBP-550 and CBR-550), and the E_a was also achieved in the stated range of 21–84 kJ mol^{-1} for the reactions of biodiesel syntheses [57, 70, 71]. According to this study, CBP-550, CBS-550, and CBR-550 catalyzed reactions have lower E_a values than the values reported by Mendonça et al. [49] (61.23 kJ mol^{-1}) and Nath et al. [57] (50.63 kJ mol^{-1}) in their studies indicating the superiority of the present catalyst.

4.6. Study of Thermodynamic Properties of the Reaction. In this study, the thermodynamic properties such as a change in enthalpy (ΔH) and entropy (ΔS) of the reactions catalyzed by CBP-550, CBS-550, and CBR-550 catalysts were calculated by using the Eyring–Polanyi equation (8). These were calculated from the intercept (ln $(k_b/h) + \Delta S/R$) and slope ($-\Delta H/R$) which was obtained by plotting the Eyring–Polanyi graph (Figure 15). The Gibbs free energy change (ΔG) for the reactions experimented at different temperatures was calculated by applying equation (9) [60].

$$\ln\left(\frac{k}{T}\right) = -\left(\frac{\Delta H}{RT}\right) + \left[\ln\left(\frac{k_b}{h}\right) + \frac{\Delta S}{R}\right], \tag{8}$$

$$\Delta G = \Delta H - T\Delta S, \tag{9}$$

where "k_b" is the Boltzmann constant ($k_b = 1.38 \times 10^{-23}$ J K^{-1}), "T" is the absolute temperature in Kelvin, and "h" is the Planck constant (h 6.626 × 10^{-34} J s).

The determined ΔH values were found to be +45.84, +41.64, and+46.54 kJ mol^{-1} K^{-1} for the reactions catalyzed by CBP-550, CBS-550, and CBR-550 catalysts, respectively (Table 8). Consequently, these positive values of the ΔH explain that the reaction takes place through an endothermic process and requires external heat to proceed [60]. Sarve et al. [73] and Nath et al. [57] also stated the positive ΔH values for biodiesel production via the transesterification process explaining that their reactions were endothermic in nature too. In the present work, the determined ΔS values were found to be negative ($\Delta S < 0$) as shown in Table 8 which indicates that the randomness occurring during the reaction is less [74]. The calculated ΔG values (Table 8) for the reactions experimented at different temperatures show that the obtained results are all positive ($\Delta G > 0$). This positive value describes that the reactions catalyzed by the present catalysts are nonspontaneous and endergonic reactions [57].

4.7. Comparison of Bharatmoni Catalysts with Other Biomass-Based Catalysts. In this work, the performances of CBP-550, CBS-550, and CBR-550 catalysts are compared with other reported catalysts and summarized in Table 9. Under the optimum experimental conditions (5 wt%, 9 : 1, 65°C), the present study disclosed that the utilization of CBP-550, CBS-550, and CBR-550 catalysts in the reaction produced the highest biodiesel yield of 96.89%, 96.97%, and 96.53%, respectively, in short reaction time. Sarma et al. [75] and Aslam et al. [76] experimented setting out a

Table 9: Catalytic activities of Bharatmoni catalysts and their comparison in biodiesel syntheses with other reported solid catalysts derived from waste biomass.

Biodiesel feedstock	Catalyst	Surface area ($m^2 g^{-1}$)	MTOMR	Parameters				References
				Catalyst (wt%)	Temp (°C)	Time (min)	Biodiesel, Y or C (%)	
J. curcas oil	CBP-550 (peel)	2.061	9 : 1	5	65	16	96.89 (Y)	This study
J. curcas oil	CBS-550 (stem)	0.730	9 : 1	5	65	12	96.97 (Y)	This study
J. curcas oil	CBR-550 (rhizome)	0.857	9 : 1	5	65	18	96.53 (Y)	This study
J. curcas oil	MBUS	38.7	9 : 1	5	275	60	98 (Y)	[75]
Waste soybean cooking oil	Sweet potato leaves	2.81	9 : 1	5	60	120	98.0 (C)	[53]
Waste cooking oil	Potato peel	23.5	9 : 1	3	60	120	97.5 (C)	[46]
J. curcas oil	*Musa champa peduncle*	8.57	12 : 1	7	65	6	98.23 (Y)	[57]
J. curcas oil	*Musa champa*	6.848	9 : 1	5	65	10	98.27 (Y)	[41]
Palm oil	Passion fruit peel	—	15 : 1	7	RT	30	95.4 (Y)	[45]
Mesua ferrea oil	MBUS	38.7	9 : 1	5	275	60	95 (C)	[76]
Soybean oil	Snail shell	7.0	6 : 1	3	28	420	98 (Y)	[77]
Waste cooking oil	*Citrus sinensis* peel ash@Fe_3O_4	15.55	6 : 1	6	65	180	98 (Y)	[56]
Soybean waste cooking oil	*Musa acuminata* peel	12	9 : 1	1.5	60	120	98 (Y)	[27]
Sunflower oil	*Sesamum indicum*	3.66	12 : 1	7	65	40	98.9 (Y)	[2]
Moringa oleifera oil	Pawpaw peel	3.6	9 : 1	3.5	35	40	96.43 (Y)	[44]
J. curcas oil	$CaCO_3$-*Acacia nilotica* ash	14.0	12 : 1	5	65	180	91.7 (C)	[51]
Soybean oil	*Moringa oleifera* leaves	—	6 : 1	6	65	120	86.7 (Y)	[78]
J. curcas oil	*Lemna perpusilla*	9.6	9 : 1	5	65	300	89.43 (Y)	[23]
Madhuca indica oil	Poovan banana pseudostem	4.58	14.9 : 1	5.9	65	178	97.97 (C)	[24]
Used vegetable oil	*Carica papaya* peel	—	12 : 1	3.5	65	60	97.5 (Y)	[21]
J. curcas oil	*Heteropanax fragrans*	27.50	12 : 1	7	65	65	97.75 (Y)	[79]
Ceiba pentandra oil	MA peduncle	45.9	11.46 : 1	2.68	65	106	98.73 (C)	[35]
Soybean oil	Orange peel ash	605.60	6 : 1	7	RT	420	98 (C)	[26]

Wt: weight; min: minute; Y: yield; Temp: temperature; C: conversion; MTOMR: methanol-to-oil molar ratio; MB: *Musa balbisiana*; MBUS: *Musa balbisiana* underground stem; MA: *Musa acuminate*.

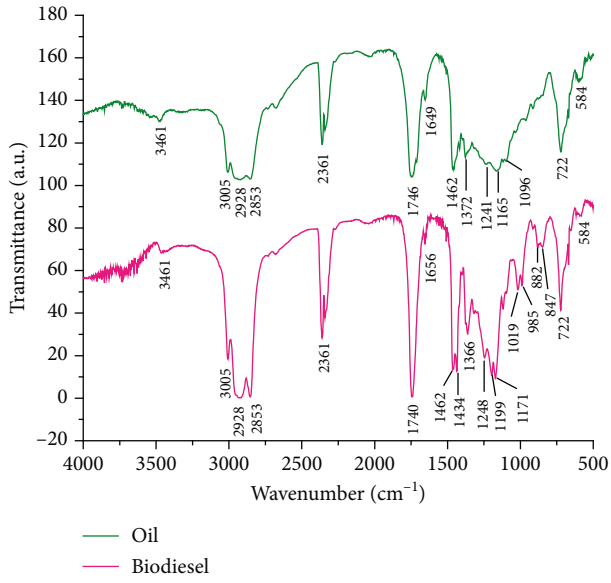

Figure 16: FT-IR spectra of *J. curcas* oil and its biodiesel.

transesterification reaction at a very high temperature (275°C) from which they achieved 98% yield in 60 min and 95% conversion in 60 min, respectively. Considering the energy input and reaction time, their catalysts are less effective than the current catalysts. Likewise, Laskar et al. [77] and Changmai et al. [56] also reported higher duration of reaction that might be due to the lower basic strength of their catalysts in comparison to the current catalysts. There are some works on the production of biodiesel from a variety of oil feedstocks applying solid base catalysts producing higher biodiesel yield than this work but reported longer reaction completion time, for example, Daimary et al. [27] achieved 98% in 120 min, Eldiehy et al. [53] obtained 98% of biodiesel in 120 min, Daimary et al. [46] reported 97.5% conversion in 120 min, and Nath et al. [2] also reported 98.9% yield in 40 min (Table 9). So, the present calcined catalysts are revealed to be better at synthesizing biodiesel faster than their catalysts. The present calcined catalysts have better catalytic activity than the catalysts studied by Tarigan et al. [45], Oladipo et al. [44], Sharma et al. [51], Aleman-Ramirez et al. [78], and Chouhan and Sarma [23] because their catalysts achieved lower biodiesel yield or conversion with longer reaction time. Niju et al. [24], Etim et al. [21], Basumatary et al. [79], Balajii and Niju [35], and Changmai et al. [26] have reported lower potassium contents causing less catalytic activity. Basumatary et al. [41] and Nath et al. [57] reported comparable catalytic activity, and their catalysts also exhibited high basic in nature due to the presence of high concentration of alkali metal carbonates and oxides. Although present catalysts have a lower surface area than the other biomass-based catalysts mentioned in Table 9, it has superior catalytic activity because of the high concentration of potassium and more basic nature. Thus, present catalysts (CBP-550, CBS-550, and CBR-550) have a significant capacity for catalyzing the transesterification for faster production of biodiesel.

4.8. FT-IR, NMR, and GC-MS Analyses. The FT-IR analyzed spectra for *J. curcas* oil and produced biodiesel are displayed in Figure 16. The strong absorption peak at 1746 cm^{-1} is attributed to the stretching frequency of C=O group of the glyceride in oil. The existence of methyl ester in the present biodiesel sample was characterized by the strong absorption peak of C=O stretching frequency at 1740 cm^{-1} which is a significant implication of the successful conversion of *J. curcas* oil into FAME [79]. Both for oil and biodiesel, the band at 3461 cm^{-1} with weak intensity is belonging to -C=O overtone. The peak located at 3005 cm^{-1} is due to = C-H stretching of -CH=CH- signifying the presence of a fatty acid chain with unsaturation. The bands at 2928 cm^{-1} and 2853 cm^{-1} indicated the =C-H asymmetric and $-CH_2$ symmetric stretching vibrations, respectively [80]. The peaks of shear-type vibration of $-CH_2$ with moderate intensity are also recognized for oil at 1462 cm^{-1} and biodiesel at 1462 and 1434 cm^{-1}. Besides that, CH_3 bending vibration displays the peaks at 1372 and 1241 cm^{-1} for oil and at 1366 and 1248 cm^{-1} for biodiesel [48, 80]. The peaks for oil at 1165 and 1096 cm^{-1} and biodiesel at 1199, 1171, and 1019 cm^{-1} indicate the antisymmetric stretching vibrations of C-O-C. It is evident that $-CH_2-$ plane rocking of long chains of fatty acids is responsible for the peak exhibiting at 722 cm^{-1} both for oil and the produced biodiesel [80]. The study exposed the transformation of *J. curcas* oil into biodiesel by revealing the above-mentioned remarkable peaks. The ^{1}H-NMR spectroscopic analysis result of *J. curcas* biodiesel of this work is displayed in Figure 17. The various protons revealed by the ^{1}H-NMR analysis at different chemical shifts can be observed, more significantly the signal appearing at δ 3.592 ppm interpreted the formation of methoxy proton ($-COOCH_3$) of esters that was found in the sample of produced biodiesel. Generally, methine proton (-CH-) at C2 of glycerides ($-CH-CO_2R$) and methylene protons ($-CH_2-$) at C1 and C3 of glycerides ($-CH_2-CO_2R$) can be found in triglyceride whereas methoxy protons of ester groups do not exist in triglyceride [41, 57, 81]. The methine proton and methylene protons were not found by the ^{1}H-NMR spectrum of biodiesel. Thus, the formation of a singlet signal for the existence of methoxy protons in the biodiesel of this work confirmed that *J. curcas* oil is successfully converted to biodiesel after transesterification. From the analyzed GC chromatograms (Figure S7) and following the library search with TurboMass software, the FAME profiles that existed in the transformed biodiesel are shown in Table 10. The analysis result confirmed that the produced biodiesel has methyl oleate (41.326%), methyl palmitate (20.105%), and methyl linoleate (17.883%) as major components along with methyl stearate (4.831%), methyl arachidate (1.290%), methyl gondoate (0.848%), and methyl lignocerate (0.177%) as minor components.

4.9. Physicochemical Properties of Biodiesel. The physicochemical properties of the generated biodiesel in this work were analyzed and compared with other biodiesel and international standards set by ASTM D6751 and EN 14214 (Table 11). The determined AV and FFA of the oil were found to be 9.2 mg KOH/g and 4.6 mg KOH/g, respectively.

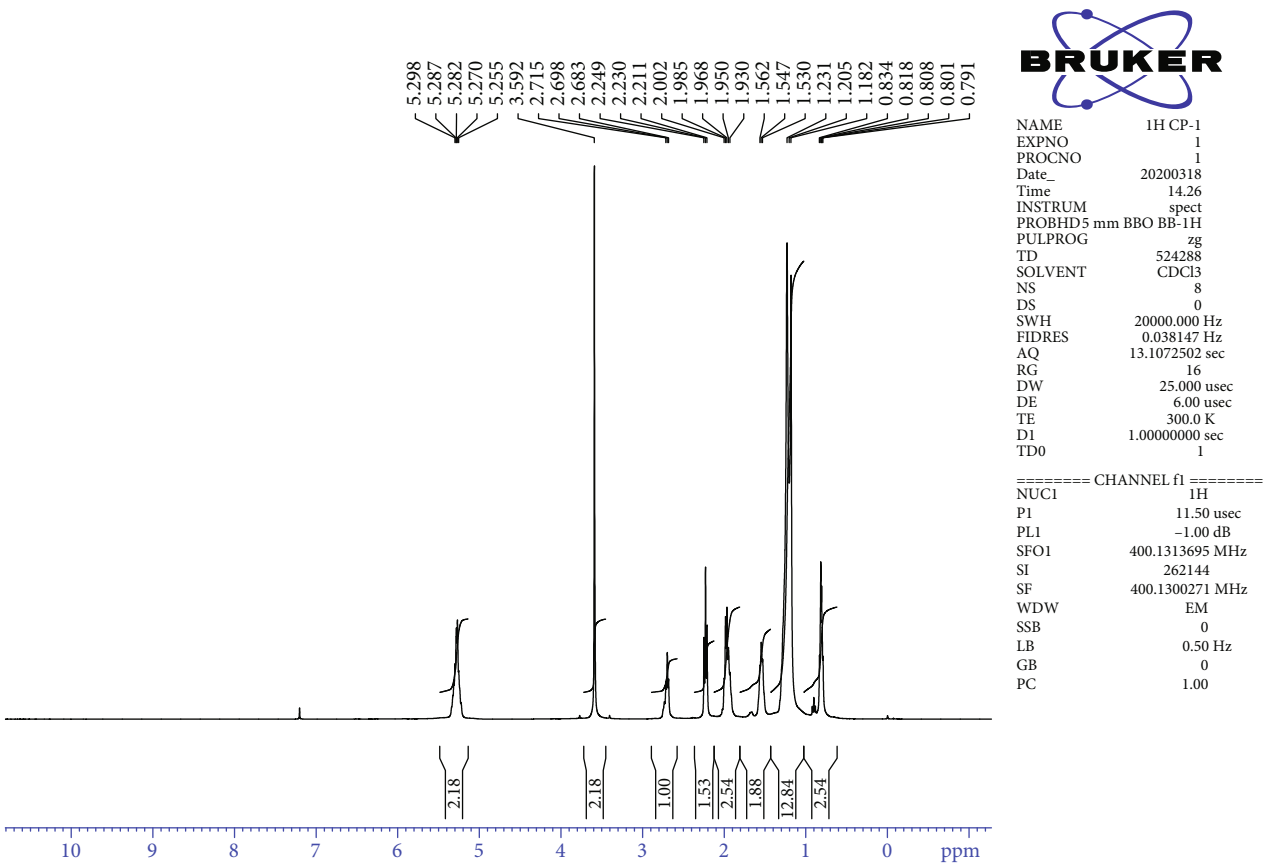

Figure 17: ^{1}H NMR spectrum of *J. curcas* biodiesel.

Table 10: Chemical compositions of *J. curcas* biodiesel from GC-MS analysis.

RT	FAME	Composition (%)
29.25	Methyl palmitate [C16:0]	20.105
31.61	Methyl linoleate [C18:2]	17.883
32.02	Methyl oleate [C18:1]	41.326
32.14	Methyl stearate [C18:0]	4.831
33.47	Methyl gondoate [C20:1]	0.848
33.70	Methyl arachidate [C20:0]	1.290
37.68	Methyl lignocerate [C24:0]	0.177

This oil feedstock was utilized to synthesize biodiesel through direct transesterification without pretreatment or esterification. The AV and FFA of the produced biodiesel showed 0.36 mg KOH/g and 0.18 mg KOH/g, respectively. This AV value of the produced biodiesel is within the maximum limit of 0.5 mg KOH/g prescribed by international standard EN 14214. Chouhan and Sarma [23] and Taufiq-Yap et al. [82] also reported the direct transesterification of *J. curcas* oil into biodiesel without pretreatment having an AV of 7.46 and 13.60 mg KOH/g, respectively. This study obtained the density of biodiesel as 0.8757 g/cm^3 at 15°C, which is within the range of standard values and well compared to other results mentioned in Table 11. Thus, in terms of density, the produced biodiesel is preferable since the density also determines how much fuel is required to generate particular engine power based on its density [35]. For biodiesel to flow smoothly through an engine, its kinematic viscosity is responsible and the value obtained for the present biodiesel is 4.027 mm^2/s at 40°C which meets the value of the international standard. This value is lower than the kinematic viscosity value determined by Chouhan and Sarma [23] and Olatundun et al. [83] which means that the present fuel has better combustion characteristics without deposition in the engine than their studies [79]. The cetane number was obtained to be 50.3, and it is above the minimal value specified by ASTM D6751 and slightly greater than the cetane number of biodiesels reported by Sarma et al. [75] and Kumar et al. [84]. The calculated cetane index for the present biodiesel is 57.58. In this study, the significant fuel property like pour point and cold filter plugging point (CFPP) of biodiesel was computed to be 0°C and <4°C, respectively. The saponification number (SN) was determined to be 191.28 (mg KOH/g) that expresses saponifiable unit per unit weight of *J. curcas* biodiesel. The iodine value representing the unsaturation degree was observed to be 76.70 g I_2/100 g which is below the stated limit of EN 14214 standard, and nearly the same values were reported by Olatundun et al. [83] and Falowo and Betiku [54], but Sarma et al. [75] achieved higher iodine value. The determined value of the diesel index, American petroleum index (API), and aniline point for the biodiesel produced in this work was recorded as 66.08, 34.28, and 192.77, respectively.

Table 11: Physicochemical properties of *J. curcas* biodiesel and comparison with standards and reported biodiesel.

Properties	Jatropha biodiesel (this study)	ASTM D6751	EN 14214	Reported biodiesel								
				Honne seed oil [83]	Jatropha oil [23]	Jatropha oil [75]	Yellow oleander-rubber oil [54]	Jatropha oil [84]	*Moringa oleifera* oil [86]	Palm kernel oil [87]	Jatropha oil [60]	*Azadirachta indica* oil [88]	WCO [46]
Density at 15°C (g/cm^3)	0.8757	0.86–0.90	0.86–0.90	870.19	0.891	0.875	0.887	0.875	0.874	—	0.874		0.88
Kinematic viscosity at 40°C (mm^2/s)	4.027	1.9–6.0	3.5–5.0	5.98	6.8	5.7	—	4.75	4.1	4.7	5.659	5.0	3.90
Cetane number	50.3	47 (min)	51 (min)	55.1126	—	48.6	55	48.3	55.56	44.4	—		52
Cetane index	57.58	NS	NS		—	—	—		—	—	58.95		—
Pour point (°C)	0	NS	NS		—	3	—	-6	-1	-3	—		-6
CFPP (°C)	<4	NS	NS		—	—	—	—	—	—	—		—
SN (mg KOH/g)	191.28	NS	NS		—	—	—	—	—	—	191.84		—
Iodine value (g I_2/100 g)	76.70	NS	120 (max)	76.14	—	119	75.65	74.5	—	24.7	70.24	58.6	—
API	34.28	36.95	NS		0.892	0.875	—	—	—	30.51	34.28		—
Diesel index	66.08	50.4	NS		—	—	—	—	—	47.87	67.98		—
Aniline point	192.77	331	—		—	—	—	—	—	—	198.33		—
HHV (MJ/kg)	40.44	NS	NS	39.66	37.100	39.25	39.70	38.35	—	—	40.51	48.7	39.80

WCO: waste cooking oil; NS: not specified; max: maximum; min: minimum; CFPP: cold filter plugging point; SN: saponification number; API: American petroleum index; HHV: higher heating value.

The energy content in the present biodiesel was measured in terms of higher heating value (HHV) and was found to be 40.44 MJ/kg which is considered as a good fuel characteristic for biodiesel.

5. Conclusion

This study has successfully derived an efficient solid catalyst with high catalytic activity from the postharvested waste of Bharatmoni for biodiesel production using *J. curcas* oil. The order of catalytic activity and biodiesel yield under the optimized conditions were found as CBS-550 (96.97% in 12 min) > CBP-550 (96.89% in 16 min) > CBR-550 (96.53% in 18 min). This reactivity order follows the trends of the amount of potassium present in the catalysts which is in the sequence of CBS-550 (46.88 wt%) > CBP-550 (44.88 wt%) > CBR-550 (39.33 wt%) from EDX analyses. The investigated pH value, basicity, and TOF values of CBS-550 are greater than those of the CBP-550 and CBR-550 catalysts, which are also the reasons for achieving the higher activity. The FESEM, BET, and HRTEM affirmed that the present calcined catalysts consist of porous materials which are primarily mesoporous. The reaction of the present work follows the kinetic model of pseudo-first-order and demonstrated an endothermic process, which is endergonic and nonspontaneous. The CBS-550 catalyst (44.36 kJ mol^{-1}) showed a lower E_a value than CBP-550 (48.56 kJ mol^{-1}) and CBR-550 (49.26 kJ mol^{-1}) catalysts. The CBS-550 catalyst showed satisfactory reusability up to the 3rd cycle with 93.20% product yield at optimized conditions. Therefore, the catalysts derived from the postharvested Bharatmoni waste are attractive and significant for their catalytic characteristics. The preparation method of the catalyst is very simple, directly applicable in transesterification, and it is nontoxic, renewable, and low-cost catalyst possessing high catalytic activity for production of biodiesel.

Nomenclature

BBP: Burnt Bharatmoni peel
BBS: Burnt Bharatmoni stem
BBR: Burnt Bharatmoni rhizome
CBP-550: Calcined Bharatmoni peel at 550°C
CBS-550: Calcined Bharatmoni stem at 550°C
CBR-550: Calcined Bharatmoni rhizome at 550°C
FT-IR: Fourier-transform infrared spectroscopy
BET: Brunauer-Emmett-Teller
FESEM: Field emission scanning electron microscope
EDX: Energy-dispersive X-ray spectroscopy
XPS: X-ray photoelectron spectroscopy
XRD: X-ray diffraction
HRTEM: High-resolution transmission electron microscope
SAED: Selected area electron diffraction
GC-MS: Gas chromatography-mass spectrometry
TLC: Thin layer chromatography
JCPDS: Joint Committee on Powder Diffraction Standards
E_a: Activation energy
NMR: Nuclear magnetic resonance
TOF: Turnover frequency
SN: Saponification number
IV: Iodine value
AV: Acid value
CFPP: Cold filter plugging point
MTOMR: Methanol-to-oil molar ratio
HHV: Higher heating value
API: American petroleum index.

Data Availability

The data used to support the findings of this study are available from the corresponding author upon request.

Conflicts of Interest

The authors declare that there are no conflicts of interest regarding the publication of this article.

Authors' Contributions

Bidangshri Basumatary was responsible for the methodology, investigation, and writing of the original draft. Alpaslan Atmanli was responsible for the validation, writing, review, and editing of the manuscript. Mohammad Azam was responsible for the validation, writing, review, and editing of the manuscript. Siri Fung Basumatary was responsible for the writing, review, and editing of the manuscript. Sujata Brahma was responsible for the writing, review, and editing of the manuscript. Bipul Das was responsible for the formal analysis and resources. Sanfaori Brahma was responsible for the resources, writing, review, and editing of the manuscript. Samuel Lalthazuala Rokhum was responsible for the validation, writing, review, and editing of the manuscript. Kim Min was responsible for the writing, review, and editing of the manuscript. Manickam Selvaraj was responsible for the validation, writing, review, and editing of the manuscript. Sanjay Basumatary was responsible for the conceptualization, methodology, supervision, writing, review, and editing of the manuscript.

Acknowledgments

The authors acknowledge MARC Bangalore, CSIR-NEIST Jorhat, SAIF NEHU, Biotech Park IIT Guwahati, and Gauhati University (Department of Chemistry) for the analyses of the catalysts. We are thankful to Bongaigaon IOCL for investigation of biodiesel properties. Bidangshri Basumatary is thankful to CSIR-HRDG for the JRF (09/1308(15429)/2022-EMR-I). The authors acknowledge the financial support through Researchers Supporting Project number RSP2024R147, King Saud University, Riyadh, Saudi Arabia. The authors also extend their appreciation to the research unit at King Khalid University for funding this work through the project number 423/44, and the authors acknowledge the Research Center for Advance Materials (RCAMS) at King Khalid University, Saudi Arabia, for their valuable technical support.

Supplementary Materials

Figure S1: pictorial representation of raw materials of Bharatmoni banana peel (A–C), stem (D–F), and rhizome (G–I) for catalyst preparation. Figure S2: FESEM images (A–C) and EDX spectrum (D) of the 3rd recycled catalyst of CBS-550. Figure S3: TEM images of CBP-550 (A, B), CBS-550 (C, D), and CBR-550 (E, F) catalysts. Figure S4: effect of temperature on biodiesel synthesis. Reaction conditions: MTOMR = 9 : 1 and catalyst loading (CBP − 550, CBS − 550, and CBR − 550) = 5 wt%. Figure S5: catalytic activities of the uncalcined Bharatmoni catalysts in biodiesel production. Reaction conditions: temperature = 65°C, MTOMR = 9 : 1, and catalyst loading (BBP, BBS, and BBR) = 5 wt%. Figure S6: reusability of CBS-550 catalyst (reaction temperature = 65°C, MTOMR = 9 : 1, and catalyst loading = 5 wt%). Figure S7: GC-MS of *J. curcas* biodiesel. *(Supplementary Materials)*

References

[1] A. L. Ahmad, N. M. Yasin, C. J. Derek, and J. K. Lim, "Microalgae as a sustainable energy source for biodiesel production: a review," *Renewable and Sustainable Energy Reviews*, vol. 15, no. 1, pp. 584–593, 2011.

[2] B. Nath, P. Kalita, B. Das, and S. Basumatary, "Highly efficient renewable heterogeneous base catalyst derived from waste *Sesamum indicum* plant for synthesis of biodiesel," *Renewable Energy*, vol. 151, pp. 295–310, 2020.

[3] S. Banerjee, S. Sahani, and Y. C. Sharma, "Process dynamic investigations and emission analyses of biodiesel produced using Sr–Ce mixed metal oxide heterogeneous catalyst," *Journal of Environmental Management*, vol. 248, article 109218, 2019.

[4] H. P. Makkar and K. Becker, "*Jatropha curcas*, a promising crop for the generation of biodiesel and value-added coproducts," *European Journal of Lipid Science and Technology*, vol. 111, no. 8, pp. 773–787, 2009.

[5] I. B. Banković-Ilić, M. R. Miladinović, O. S. Stamenković, and V. B. Veljković, "Application of nano CaO-based catalysts in biodiesel synthesis," *Renewable and Sustainable Energy Reviews*, vol. 72, pp. 746–760, 2017.

[6] C. E. Akhabue, E. O. Osa-Benedict, E. A. Oyedoh, and S. K. Otoikhian, "Development of a bio-based bifunctional catalyst for simultaneous esterification and transesterification of neem seed oil: modeling and optimization studies," *Renewable Energy*, vol. 152, pp. 724–735, 2020.

[7] S. F. Ibrahim, N. Asikin-Mijan, M. L. Ibrahim, G. Abdulkareem-Alsultan, S. M. Izham, and Y. H. Taufiq-Yap, "Sulfonated functionalization of carbon derived corncob residue via hydrothermal synthesis route for esterification of palm fatty acid distillate," *Energy Conversion and Management*, vol. 210, article 112698, 2020.

[8] N. N. Yusuf, S. K. Kamarudin, and Z. Yaakob, "Overview on the production of biodiesel fromJatropha curcasL. by using heterogenous catalysts," *Biofuels, Bioproducts and Biorefining*, vol. 6, no. 3, pp. 319–334, 2012.

[9] A. A. de Jesus, D. F. de Santana Souza, J. A. de Oliveira et al., "Mathematical modeling and experimental esterification at supercritical conditions for biodiesel production in a tubular reactor," *Energy Conversion and Management*, vol. 171, pp. 1697–1703, 2018.

[10] M. Tariq, S. Ali, and N. Khalid, "Activity of homogeneous and heterogeneous catalysts, spectroscopic and chromatographic characterization of biodiesel: a review," *Renewable and Sustainable Energy Reviews*, vol. 16, no. 8, pp. 6303–6316, 2012.

[11] K. G. Georgogianni, A. K. Katsoulidis, P. J. Pomonis, G. Manos, and M. G. Kontominas, "Transesterification of rapeseed oil for the production of biodiesel using homogeneous and heterogeneous catalysis," *Fuel Processing Technology*, vol. 90, no. 7-8, pp. 1016–1022, 2009.

[12] M. Yadav, V. Singh, and Y. C. Sharma, "Methyl transesterification of waste cooking oil using a laboratory synthesized reusable heterogeneous base catalyst: process optimization and homogeneity study of catalyst," *Energy Conversion and Management*, vol. 148, pp. 1438–1452, 2017.

[13] M. K. Lam, K. T. Lee, and A. R. Mohamed, "Homogeneous, heterogeneous and enzymatic catalysis for transesterification of high free fatty acid oil (waste cooking oil) to biodiesel: a review," *Biotechnology Advances*, vol. 28, no. 4, pp. 500–518, 2010.

[14] S. H. Abdullah, N. H. Hanapi, A. Azid et al., "A review of biomass-derived heterogeneous catalyst for a sustainable biodiesel production," *Renewable and Sustainable Energy Reviews*, vol. 70, pp. 1040–1051, 2017.

[15] N. S. Talha and S. Sulaiman, "Overview of catalysts in biodiesel production," *ARPN Journal of Engineering and Applied Sciences*, vol. 11, pp. 439–442, 2016.

[16] A. M. Dehkordi and M. Ghasemi, "Transesterification of waste cooking oil to biodiesel using Ca and Zr mixed oxides as heterogeneous base catalysts," *Fuel Processing Technology*, vol. 97, pp. 45–51, 2012.

[17] I. B. Laskar, R. Gupta, S. Chatterjee, C. Vanlalveni, and L. Rokhum, "Taming waste: waste *Mangifera indica* peel as a sustainable catalyst for biodiesel production at room temperature," *Renewable Energy*, vol. 161, pp. 207–220, 2020.

[18] S. Basumatary, B. Nath, and P. Kalita, "Application of agro-waste derived materials as heterogeneous base catalysts for biodiesel synthesis," *Journal of Renewable and Sustainable Energy*, vol. 10, no. 4, article 043105, 2018.

[19] B. Nath, B. Das, P. Kalita, and S. Basumatary, "Waste to value addition: utilization of waste *Brassica nigra* plant derived novel green heterogeneous base catalyst for effective synthesis of biodiesel," *Journal of Cleaner Production*, vol. 239, article 118112, 2019.

[20] G. Pathak, D. Das, K. Rajkumari, and S. L. Rokhum, "Exploiting waste: towards a sustainable production of biodiesel using *Musa acuminata* peel ash as a heterogeneous catalyst," *Green Chemistry*, vol. 20, no. 10, pp. 2365–2373, 2018.

[21] A. O. Etim, A. C. Eloka-Eboka, and P. Musonge, "Potential of *Carica papaya* peels as effective biocatalyst in the optimized parametric transesterification of used vegetable oil," *Environmental Engineering Research*, vol. 26, no. 4, 2021.

[22] M. Gohain, K. Laskar, H. Phukon, U. Bora, D. Kalita, and D. Deka, "Towards sustainable biodiesel and chemical production: multifunctional use of heterogeneous catalyst from littered *Tectona grandis* leaves," *Waste Management*, vol. 102, pp. 212–221, 2020.

[23] A. P. Chouhan and A. K. Sarma, "Biodiesel production from *Jatropha curcas* L. oil using *Lemna perpusilla* Torrey ash as heterogeneous catalyst," *Biomass and Bioenergy*, vol. 55, pp. 386–389, 2013.

[24] S. Niju, A. Janaranjani, R. Nanthini, P. A. Sindhu, and M. Balajii, "Valorization of banana pseudostem as a catalyst

for transesterification process and its optimization studies," *Biomass Conversion and Biorefinery*, vol. 13, no. 3, pp. 1805–1818, 2023.

[25] I. B. Laskar, T. Deshmukhya, A. Biswas et al., "Utilization of biowaste-derived catalysts for biodiesel production: process optimization using response surface methodology and particle swarm optimization method," *Energy Adv.*, vol. 1, no. 5, pp. 287–302, 2022.

[26] B. Changmai, P. Sudarsanam, and L. Rokhum, "Biodiesel production using a renewable mesoporous solid catalyst," *Industrial Crops and Products*, vol. 145, article 111911, 2020.

[27] N. Daimary, P. Boruah, K. S. Eldiehy et al., "*Musa acuminata* peel: a bioresource for bio-oil and by-product utilization as a sustainable source of renewable green catalyst for biodiesel production," *Renewable Energy*, vol. 187, pp. 450–462, 2022.

[28] D. Mohapatra, S. Mishra, and N. Sutar, "Banana and its by-product utilization: an overview," *Journal of Scientific and Industrial Research*, vol. 69, pp. 323–329, 2010.

[29] M. K. Kumar, B. M. Muralidhara, M. U. Rani, and J. A. Gowda, "A figuration of banana production in India," *Environment and Ecology*, vol. 31, pp. 1860–1862, 2013.

[30] H. Pyar and K. K. Peh, "Chemical compositions of banana peels (*Musa sapientum*) fruits cultivated in Malaysia using proximate analysis," *Research Journal of Chemistry and Environment*, vol. 22, pp. 108–111, 2018.

[31] M. Balajii and S. Niju, "A novel biobased heterogeneous catalyst derived from *Musa acuminata* peduncle for biodiesel production–process optimization using central composite design," *Energy Conversion and Management*, vol. 189, pp. 118–131, 2019.

[32] E. Betiku, A. M. Akintunde, and T. V. Ojumu, "Banana peels as a biobase catalyst for fatty acid methyl esters production using Napoleon's plume (*Bauhinia monandra*) seed oil: a process parameters optimization study," *Energy*, vol. 103, pp. 797–806, 2016.

[33] M. Gohain, A. Devi, and D. Deka, "*Musa balbisiana* Colla peel as highly effective renewable heterogeneous base catalyst for biodiesel production," *Industrial Crops and Products*, vol. 109, pp. 8–18, 2017.

[34] E. Betiku and S. O. Ajala, "Modeling and optimization of *Thevetia peruviana* (yellow oleander) oil biodiesel synthesis via *Musa paradisiacal* (plantain) peels as heterogeneous base catalyst: a case of artificial neural network vs. response surface methodology," *Industrial Crops and Products*, vol. 53, pp. 314–322, 2014.

[35] M. Balajii and S. Niju, "Banana peduncle–a green and renewable heterogeneous base catalyst for biodiesel production from *Ceiba pentandra* oil," *Renewable Energy*, vol. 146, pp. 2255–2269, 2020.

[36] M. Fan, H. Wu, M. Shi, P. Zhang, and P. Jiang, "Well-dispersive K_2OKCl alkaline catalyst derived from waste banana peel for biodiesel synthesis," *Green Energy & Environment*, vol. 4, no. 3, pp. 322–327, 2019.

[37] T. Ahmad and M. Danish, "Prospects of banana waste utilization in wastewater treatment: a review," *Journal of Environmental Management*, vol. 206, pp. 330–348, 2018.

[38] B. Nath, B. Basumatary, N. Wary et al., "Agricultural waste-based heterogeneous catalyst for the production of biodiesel: a ranking study via the VIKOR method," *International Journal of Energy Research*, vol. 2023, Article ID 7208754, 23 pages, 2023.

[39] K. Borborah, D. Saikia, M. Rehman et al., "Comparative analysis of genetic diversity in some non-commercial cultivars of *Musa* L. from Assam, India, using morphometric and ISSR markers," *International Journal of Fruit Science*, vol. 20, pp. 1814–1828, 2020.

[40] A. Saikia, P. Kalita, S. H. Devi et al., "Water deficit implication on the growth attributing characters of some selected improved banana germplasm under in an Inseptisol of North East India," *International Research Journal of Pure and Applied Chemistry*, vol. 21, pp. 53–65, 2020.

[41] B. Basumatary, S. Brahma, B. Nath, S. F. Basumatary, B. Das, and S. Basumatary, "Post-harvest waste to value-added materials: *Musa champa* plant as renewable and highly effective base catalyst for *Jatropha curcas* oil-based biodiesel production," *Bioresource Technology Reports*, vol. 21, article 101338, 2023.

[42] S. Basumatary, P. Barua, and D. C. Deka, "*Gmelina arborea* and *Tabernaemontana divaricata* seed oils as non-edible feedstocks for biodiesel production," *International Journal of ChemTech Research*, vol. 6, pp. 1440–1445, 2014.

[43] T. F. Adepoju, B. E. Olatunbosun, O. M. Olatunji, and M. A. Ibeh, "Brette pearl spar mable (BPSM): a potential recoverable catalyst as a renewable source of biodiesel from *Thevetia peruviana* seed oil for the benefit of sustainable development in West Africa," *Energy, Sustainability and Society*, vol. 8, no. 1, pp. 1–7, 2018.

[44] B. Oladipo, T. V. Ojumu, L. M. Latinwo, and E. Betiku, "Pawpaw (*Carica papaya*) peel waste as a novel green heterogeneous catalyst for moringa oil methyl esters synthesis: process optimization and kinetic study," *Energies*, vol. 13, no. 21, p. 5834, 2020.

[45] J. B. Tarigan, K. Singh, J. S. Sinuraya et al., "Waste passion fruit peel as a heterogeneous catalyst for room-temperature biodiesel production," *ACS Omega*, vol. 7, no. 9, pp. 7885–7892, 2022.

[46] N. Daimary, K. S. Eldiehy, P. Boruah, D. Deka, U. Bora, and B. K. Kakati, "Potato peels as a sustainable source for biochar, bio-oil and a green heterogeneous catalyst for biodiesel production," *Journal of Environmental Chemical Engineering*, vol. 10, no. 1, article 107108, 2022.

[47] M. John, M. O. Abdullah, T. Y. Hua, and C. Nolasco-Hipólito, "Techno-economical and energy analysis of sunflower oil biodiesel synthesis assisted with waste ginger leaves derived catalysts," *Renewable Energy*, vol. 168, pp. 815–828, 2021.

[48] O. A. Falowo, T. V. Ojumu, O. Pereao, and E. Betiku, "Sustainable biodiesel synthesis from honne-rubber-neem oil blend with a novel mesoporous base catalyst synthesized from a mixture of three agrowastes," *Catalysts*, vol. 10, no. 2, p. 190, 2020.

[49] I. M. Mendonça, O. A. Paes, P. J. Maia et al., "New heterogeneous catalyst for biodiesel production from waste tucumã peels (*Astrocaryum aculeatum* Meyer): parameters optimization study," *Renewable Energy*, vol. 130, pp. 103–110, 2019.

[50] J. Wang, L. Yang, W. Luo et al., "Sustainable biodiesel production via transesterification by using recyclable $Ca_2MgSi_2O_7$ catalyst," *Fuel*, vol. 196, pp. 306–313, 2017.

[51] M. Sharma, A. A. Khan, S. K. Puri, and D. K. Tuli, "Wood ash as a potential heterogeneous catalyst for biodiesel synthesis," *Biomass and Bioenergy*, vol. 41, pp. 94–106, 2012.

[52] M. R. Miladinović, M. V. Zdujić, D. N. Veljović et al., "Valorization of walnut shell ash as a catalyst for biodiesel production," *Renewable Energy*, vol. 147, pp. 1033–1043, 2020.

[53] K. S. Eldiehy, N. Daimary, D. Borah et al., "Towards biodiesel sustainability: waste sweet potato leaves as a green heterogeneous catalyst for biodiesel production using microalgal oil and waste cooking oil," *Industrial Crops and Products*, vol. 187, article 115467, 2022.

[54] O. A. Falowo and E. Betiku, "A novel heterogeneous catalyst synthesis from agrowastes mixture and application in transesterification of yellow oleander-rubber oil: optimization by Taguchi approach," *Fuel*, vol. 312, article 122999, 2022.

[55] E. Betiku, A. A. Okeleye, N. B. Ishola, A. S. Osunleke, and T. V. Ojumu, "Development of a novel mesoporous biocatalyst derived from kola nut pod husk for conversion of Kariya seed oil to methyl esters: a case of synthesis, modeling and optimization studies," *Catalysis Letters*, vol. 149, no. 7, pp. 1772–1787, 2019.

[56] B. Changmai, R. Rano, C. Vanlalveni, and L. Rokhum, "A novel *Citrus sinensis* peel ash coated magnetic nanoparticles as an easily recoverable solid catalyst for biodiesel production," *Fuel*, vol. 286, article 119447, 2021.

[57] B. Nath, B. Basumatary, S. Brahma et al., "*Musa champa* peduncle waste-derived efficient catalyst: studies of biodiesel synthesis, reaction kinetics and thermodynamics," *Energy*, vol. 270, article 126976, 2023.

[58] S. Brahma, B. Basumatary, S. F. Basumatary et al., "Biodiesel production from quinary oil mixture using highly efficient *Musa chinensis* based heterogeneous catalyst," *Fuel*, vol. 336, article 127150, 2023.

[59] K. J. Tamuli, R. K. Sahoo, and M. Bordoloi, "Biocatalytic green alternative to existing hazardous reaction media: synthesis of chalcone and flavone derivativesviathe Claisen–Schmidt reaction at room temperature," *New Journal of Chemistry*, vol. 44, no. 48, pp. 20956–20965, 2020.

[60] B. Basumatary, B. Das, B. Nath, and S. Basumatary, "Synthesis and characterization of heterogeneous catalyst from sugarcane bagasse: production of Jatropha seed oil methyl esters," *Current Research in Green and Sustainable Chemistry*, vol. 4, article 100082, 2021.

[61] I. M. Mendonça, F. L. Machado, C. C. Silva et al., "Application of calcined waste cupuaçu (*Theobroma grandiflorum*) seeds as a low-cost solid catalyst in soybean oil ethanolysis: statistical optimization," *Energy Conversion and Management*, vol. 200, article 112095, 2019.

[62] S. D. Barros, W. A. Junior, I. S. Sá et al., "Pineapple (*Ananás comosus*) leaves ash as a solid base catalyst for biodiesel synthesis," *Bioresource Technology*, vol. 312, article 123569, 2020.

[63] S. Sahani, T. Roy, and Y. C. Sharma, "Clean and efficient production of biodiesel using barium cerate as a heterogeneous catalyst for the biodiesel production; kinetics and thermodynamic study," *Journal of Cleaner Production*, vol. 237, article 117699, 2019.

[64] T. Roy, S. Sahani, and Y. C. Sharma, "Green synthesis of biodiesel from *Ricinus communis* oil (castor seed oil) using potassium promoted lanthanum oxide catalyst: kinetic, thermodynamic and environmental studies," *Fuel*, vol. 274, article 117644, 2020.

[65] M. Roy and K. Mohanty, "Valorization of de-oiled microalgal biomass as a carbon-based heterogeneous catalyst for a sustainable biodiesel production," *Bioresource Technology*, vol. 337, article 125424, 2021.

[66] S.H Dhawane, T. Kumar, and G. Halder, "Biodiesel synthesis from Hevea brasiliensis oil employing carbon supported heterogeneous catalyst: Optimization by Taguchi method," *Renewable Energy*, vol. 89, pp. 506–514, 2016.

[67] M. Hassani, G. D. Najafpour, and M. Mohammadi, "Transesterification of waste cooking oil to biodiesel using γ-alumina coated on zeolite pellets," *Journal of Materials and Environmental Science*, vol. 7, pp. 1193–1203, 2016.

[68] R. Madhuvilakku, R. Mariappan, S. Jeyapal, S. Sundar, and S. Piraman, "Transesterification of palm oil catalyzed by fresh water bivalve mollusk (*Margaritifera falcata*) shell as heterogeneous catalyst," *Industrial and Engineering Chemistry Research*, vol. 52, no. 49, pp. 17407–17413, 2013.

[69] K. Rajkumari and L. Rokhum, "A sustainable protocol for production of biodiesel by transesterification of soybean oil using banana trunk ash as a heterogeneous catalyst," *Biomass Conversion and Biorefinery*, vol. 10, no. 4, pp. 839–848, 2020.

[70] N. Y. Yahya, N. Ngadi, S. Wong, and O. Hassan, "Transesterification of used cooking oil (UCO) catalyzed by mesoporous calcium titanate: kinetic and thermodynamic studies," *Energy Conversion and Management*, vol. 164, pp. 210–218, 2018.

[71] M. Kaur, R. Malhotra, and A. Ali, "Tungsten supported Ti/SiO_2 nanoflowers as reusable heterogeneous catalyst for biodiesel production," *Renewable Energy*, vol. 116, pp. 109–119, 2018.

[72] M. A. Farid, M. A. Hassan, Y. H. Taufiq-Yap et al., "Kinetic and thermodynamic of heterogeneously K_3PO_4/AC-catalysed transesterification via pseudo-first order mechanism and Eyring-Polanyi equation," *Fuel*, vol. 232, pp. 653–658, 2018.

[73] A. N. Sarve, M. N. Varma, and S. S. Sonawane, "Ultrasound assisted two-stage biodiesel synthesis from non-edible Schleichera triguga oil using heterogeneous catalyst: kinetics and thermodynamic analysis," *Ultrasonics Sonochemistry*, vol. 29, pp. 288–298, 2016.

[74] T. Roy, S. Sahani, D. Madhu, and Y. C. Sharma, "A clean approach of biodiesel production from waste cooking oil by using single phase $BaSnO_3$ as solid base catalyst: mechanism, kinetics & e-study," *Journal of Cleaner Production*, vol. 265, article 121440, 2020.

[75] A. K. Sarma, P. Kumar, M. Aslam, and A. P. Chouhan, "Preparation and characterization of *Musa balbisiana* Colla underground stem nano-material for biodiesel production under elevated conditions," *Catalysis Letters*, vol. 144, no. 7, pp. 1344–1353, 2014.

[76] M. Aslam, P. Saxena, and A. K. Sarma, "Green technology for biodiesel production from *Mesua ferrea* L. seed oil," *Energy and Environment Research*, vol. 4, pp. 11–21, 2014.

[77] I. B. Laskar, K. Rajkumari, R. Gupta, S. Chatterjee, B. Paul, and L. Rokhum, "Waste snail shell derived heterogeneous catalyst for biodiesel production by the transesterification of soybean oil," *RSC Advances*, vol. 8, no. 36, pp. 20131–20142, 2018.

[78] J. L. Aleman-Ramirez, J. Moreira, S. Torres-Arellano, A. Longoria, P. U. Okoye, and P. J. Sebastian, "Preparation of a heterogeneous catalyst from moringa leaves as a sustainable precursor for biodiesel production," *Fuel*, vol. 284, article 118983, 2021.

[79] S. Basumatary, B. Nath, B. Das, P. Kalita, and B. Basumatary, "Utilization of renewable and sustainable basic heterogeneous catalyst from *Heteropanax fragrans* (Kesseru) for effective synthesis of biodiesel from *Jatropha curcas* oil," *Fuel*, vol. 286, article 119357, 2021.

[80] S. M. Dharma, H. H. Masjuki, H. C. Ong et al., "Optimization of biodiesel production process for mixed *Jatropha curcas*–

Ceiba pentandra biodiesel using response surface methodology," *Energy Conversion and Management*, vol. 115, pp. 178–190, 2016.

[81] B. Basumatary, S. Basumatary, B. Das, B. Nath, and P. Kalita, "Waste *Musa paradisiaca* plant: an efficient heterogeneous base catalyst for fast production of biodiesel," *Journal of Cleaner Production*, vol. 305, article 127089, 2021.

[82] Y. H. Taufiq-Yap, S. H. Teo, U. Rashid, A. Islam, M. Z. Hussien, and K. T. Lee, "Transesterification of *Jatropha curcas* crude oil to biodiesel on calcium lanthanum mixed oxide catalyst: effect of stoichiometric composition," *Energy Conversion and Management*, vol. 88, pp. 1290–1296, 2014.

[83] E. A. Olatundun, O. O. Borokini, and E. Betiku, "Cocoa pod husk-plantain peel blend as a novel green heterogeneous catalyst for renewable and sustainable honne oil biodiesel synthesis: a case of biowastes-to-wealth," *Renewable Energy*, vol. 166, pp. 163–175, 2020.

[84] P. Kumar, A. K. Sarma, A. Bansal, and M. K. Jha, "Formulation of SrO-MBCUS agglomerates for esterification and transesterification of high FFA vegetable oil," *Bulletin of Chemical Reaction Engineering & Catalysis*, vol. 11, no. 2, pp. 140–150, 2016.

[85] C. Li, X. Hu, W. M. Feng, B. Wu, and K. Wu, "A supported solid base catalyst synthesized from green biomass ash for biodiesel production," *Energy Sources, Part A: Recovery, Utilization, and Environmental Effects*, vol. 40, no. 2, pp. 142–147, 2018.

[86] R. Foroutan, S. J. Peighambardoust, R. Mohammadi, S. H. Peighambardoust, and B. Ramavandi, "Application of walnut shell ash/ZnO/K_2CO_3 as a new composite catalyst for biodiesel generation from *Moringa oleifera* oil," *Fuel*, vol. 311, article 122624, 2022.

[87] V. O. Odude, A. J. Adesina, O. O. Oyetunde et al., "Application of agricultural waste-based catalysts to transesterification of esterified palm kernel oil into biodiesel: a case of banana fruit peel versus cocoa pod husk," *Waste and Biomass Valorization*, vol. 10, no. 4, pp. 877–888, 2019.

[88] A. O. Etim, E. Betiku, S. O. Ajala, P. J. Olaniyi, and T. V. Ojumu, "Potential of ripe plantain fruit peels as an ecofriendly catalyst for biodiesel synthesis: optimization by artificial neural network integrated with genetic algorithm," *Sustainability*, vol. 10, no. 3, p. 707, 2018.